Tectonophysics 638 (2015) 63–81

Contents lists available at ScienceDirect

Tectonophysics

journal homepage: www.elsevier.com/locate/tecto

Complex local Moho topography in the Western Carpathians: Indication of the ALCAPA and the European Plate contact

Pavla Hrubcová [a,*], Piotr Środa [b]

[a] Institute of Geophysics, Academy of Sciences of the Czech Republic, 141 31 Prague, Czech Republic
[b] Institute of Geophysics, Polish Academy of Sciences, Ks. Janusza 64, 01–452 Warsaw, Poland

ARTICLE INFO

Article history:
Received 1 March 2014
Received in revised form 1 October 2014
Accepted 13 October 2014
Available online 29 October 2014

Keywords:
Western Carpathians
Seismic modelling
Crustal structure
Anomalous Moho
Bohemian Massif
Pannonian Basin

ABSTRACT

Seismic data from deep refraction and wide-angle reflection profiles intersecting the Western Carpathians show distinct upper-mantle *Pn* phases with anomalous apparent velocities identified in the first and later arrivals. Their systematic analysis indicates that such phases are present in numerous seismic sections both for in-line and off-line shots. They are observed in data from profiles intersecting the Carpathians in the west at the contact with the Bohemian Massif; similar feature was also found in data at the northern edge of the Carpathians at the contact with the North European Platform. Modelling of these anomalous *Pn* phases shows that they originate due to local structural anomalies of the Moho discontinuity detected in several places along the Western Carpathian arc. Such anomalies are located in close lateral proximity of the Pieniny Klippen Belt representing the contact between the stable European Plate in the north and the ALCAPA (Alpine–Carpathian–Pannonian) microplate in the south. Thus, the complex local Moho topography modelled from the *Pn* phases suggests tectonic relation to the formation of the Carpathian orogen. The result is supported by correlation with the large-scale Carpathian conductivity anomaly modelled in the Carpathians at a mid-crustal level. Relative lateral position of these two structures together with the Pieniny Klippen Belt at the surface delineates a zone affected by deformations at various depths along the whole Western Carpathian arc.

1. Introduction

The Moho is the outermost seismic discontinuity in the Earth and defines the base of the crust. It ranges in depth from about 3 km at ocean ridges to about 70 km in collisional orogens. This discontinuity represents a boundary between the crust and the mantle and is marked by an abrupt change of seismic *P*-wave velocity from less than ~7.2 km/s to more than ~7.8 km/s. Since the composition of the crust is different from the composition of the mantle, the Moho represents the striking evidence of a differentiation in the Earth.

The seismic signature of the Moho depends, to a large degree, on seismic methodology which was used to obtain the image. Controlled source studies reveal the Moho as a sharp refraction velocity contrast, while the Moho in normal incidence seismic reflection imaging is observed either as a reflective horizon or as an abrupt decrease of lower crustal seismic reflectivity. The characteristics of the Moho boundary depend on geology and tectonic evolution of the area. Detailed seismic reflection and refraction studies indicate it is not a simple boundary worldwide but in some regions, especially at plate or former plate boundaries, the Moho is complicated and forms a relatively complex transition zone. It can be steeply dipping at contact of plates of different age (e.g., Grad et al., 2003a,b; Hauser et al., 2007), it can be masked by reflectivity in the lower crust (e.g., Hrubcová and Geissler, 2009; Jensen et al., 2002; Thybo and Nielsen, 2012) or, as in collisional orogens, it can be offset by complex crustal faults. An example of this situation is documented in the Himalayan orogen where a 20 km offset of the Moho was recognized beneath the Indus suture, which was interpreted as a result of crustal slices thrust on top of each other during the Himalayan collision (Hirn et al., 1984a,b).

The Western Carpathians as the northernmost segment of the Alpine orogenic belt represent another example of the collisional tectonics where a complicated signature of the Moho can be expected. They originated due to continental compression in central Europe and form an arc-shaped mountain range related to the Alpine deformation during the Cretaceous to Tertiary. Difficulties in the Moho determination were firstly recognized at the western edge of the Western Carpathians by Zátopek and Beránek (1975) and Beránek and Zátopek (1981) who interpreted a broader complex zone with undisclosed pattern of the Moho topography. They detected different crustal thickness on both sides of tectonic plates but their methodology was not able to infer details of the Moho topography at a place of the contact.

* Corresponding author. Tel.: +420 267103070.
E-mail address: pavla@ig.cas.cz (P. Hrubcová).

http://dx.doi.org/10.1016/j.tecto.2014.10.013

Vast amount of data from several seismic refraction and wide angle reflection experiments recently acquired in the Western Carpathians — CELEBRATION 2000, ALP 2002 and SUDETES 2003 (Brückl et al., 2003; Grad et al., 2003a,b; Guterch et al., 2003) enables more intensive studies of this region. Modelling of data from these experiments provides constraints for seismic velocities of the crust and upper mantle in the Carpathians and the surrounding tectonic units. The seismic data recorded with high resolution and unified methodology enable not only to model robust features but also to concentrate on more complicated structural phenomena such as local complexity of the Moho and its local topography along the Western Carpathian arc.

The Moho in regional seismic refraction studies is usually detected as a relatively well defined structure with marked lateral continuity. Its topography is inferred from the wide angle reflected *PmP* phases complemented by modelling of the refracted uppermost mantle *Pn* phases. In the Western Carpathians, at their contact with surrounding tectonic units, the anomalous *Pn* phases were identified in the seismic wavefields. These phases were detected not only in the first arrivals but also with continuation to later arrivals. Such phases are not an isolated phenomenon confined to only one profile, but they are present in numerous seismic sections both for in-line and off-line shot points at different profiles. However, their systematic analysis is still missing.

In this study, we concentrate on the interpretation of the anomalous *Pn* phases using both kinematic and dynamic seismic approaches with ray tracing and full waveform modelling. This enables to locate and determine the shape of the structure at the Moho generating the anomalous phases. We discuss possible origin of such structure and compare it with results from previous geophysical studies. Since local changes in the Moho topography have tectonic significance, such investigation presents interpretational challenge to trace former tectonic plate boundaries at depth. In the Western Carpathians, knowledge about the course of tectonic suture to depth is missing, thus results from this study can shed light on tectonic evolution of the orogen.

2. Geology and tectonic setting

The Western Carpathians represent the northernmost part of the Alpine orogenic belt in Europe. They form a northward-convex arc consolidated as a result of series of Jurassic to Tertiary subduction and collision events during the Alpine orogeny (McCann, 2008). Their geological evolution is related to the convergence of plates with southward subduction of oceanic domains taking place between stable European Plate in the north and mobile fragments of continental lithosphere of the ALCAPA (Alpine–Carpathian–Pannonian) microplate in the south (Plašienka et al., 1997). The northern foreland of the Carpathians, the European Plate, encompasses the North European Platform with the Małopolska Block consolidated in Paleozoic, and the Precambrian East European Platform. To the west, the stable European Plate is formed by the Variscan Bohemian Massif consolidated during the Paleozoic with older autochthonous Brunovistulian Block (Tomek and Hall, 1993) (Fig. 1).

The Carpathian region is characterized by an arcuate orogenic belt (the Carpathians) with an extensional basin inside (the Pannonian Basin). The collisional belt of the Western Carpathians consists of the external and internal structural zones, i.e., Outer Western Carpathians and Inner Western Carpathians, respectively (McCann, 2008). The

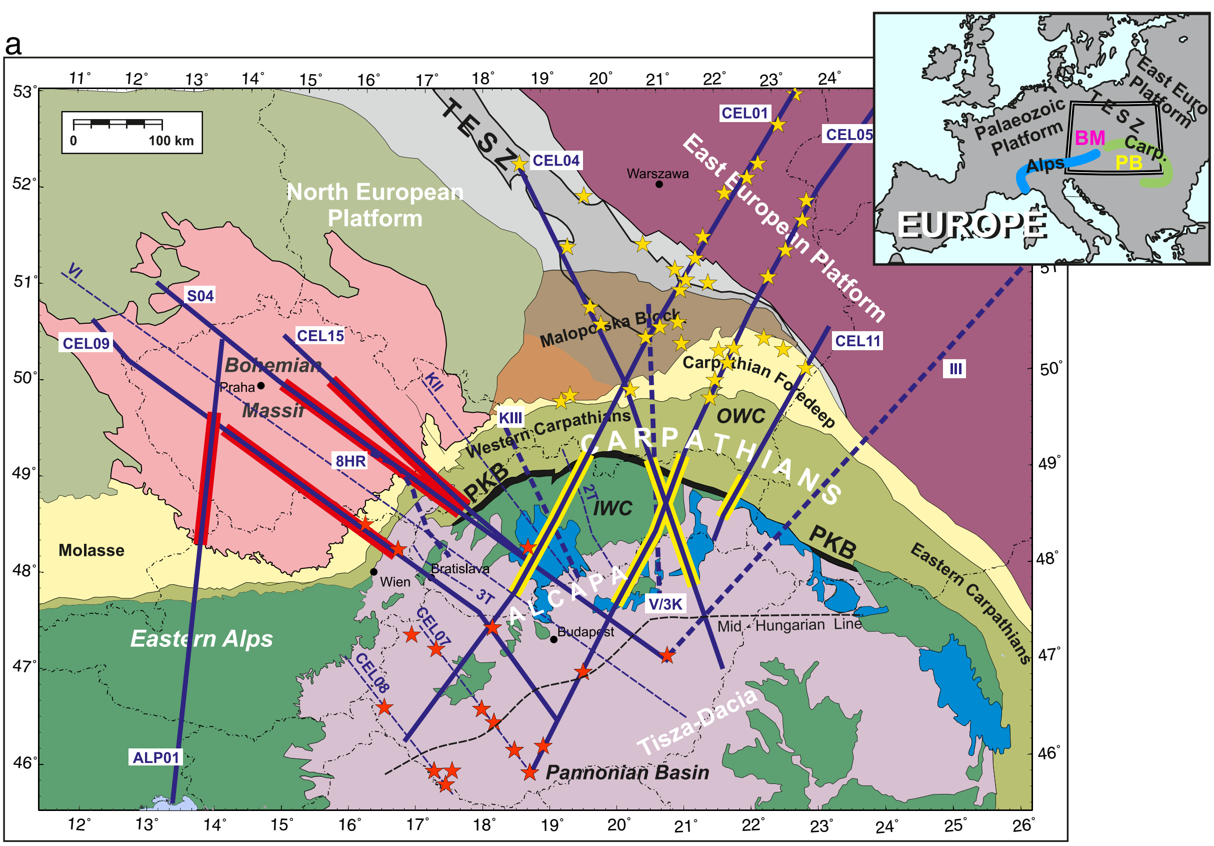

Fig. 1. (a) Simplified tectonic map of central Europe with superimposed seismic profiles from refraction and wide-angle reflection experiments CELEBRATION 2000, ALPS 2002 and SUDETES 2003 used for the interpretation of the anomalous *Pn* phases (solid lines). Other reflection and refraction profiles (dashed lines). Stars represent shot points; thick lines represent stations with anomalous upper-mantle phases (in the west marked in red, in the north marked in yellow). BM, Bohemian Massif; PB, Pannonian Basin; TESZ, Trans-European Suture Zone; OWC, Outer Western Carpathians; IWC, Inner Western Carpathians; PKB, Pieniny Klippen Belt. (b) Geographical map with refraction and wide angle reflection profiles CELEBRATION 2000, ALP 2002 and SUDETES 2003 used for the interpretation (solid lines); other reflection and refraction profiles (dashed lines). Stars represent shot points and thick lines represent stations with anomalous *Pn* phases (in the west marked in red, in the north marked in blue). Numbering refers to shot points discussed in the text.

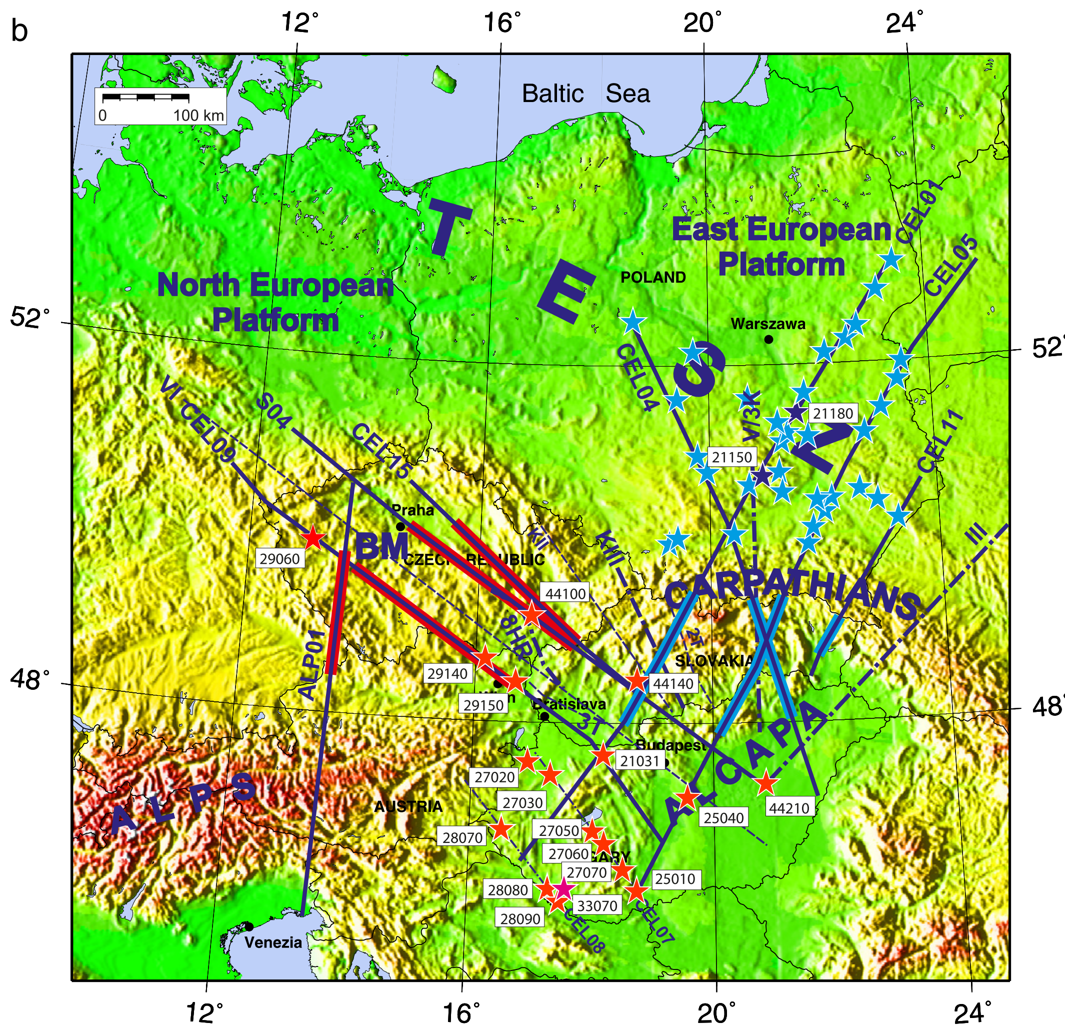

Fig. 1 (*continued*).

Outer Western Carpathians include the Carpathian Flysch Belt composed of several north-west, north, and north-east verging nappes, and the Carpathian Foredeep as the eastern/northern extension of the Alpine Molasse Basin filled by the Neogene strata. The Inner Western Carpathians were subject to extensive crustal shortening (Plašienka et al., 1997) and include various pre-Tertiary units partially covered by Tertiary sediments of the Pannonian Basin System and Neogene volcanic complexes (Fig. 1). The volcanics are represented by rhyolites and dacites related to early back-arc spreading, island-arc type andesites connected with the retreating subduction of the oceanic lithosphere beneath the Inner Western Carpathians, and alkali basalts originated due to post-subduction extension and asthenosphere updoming in the Pannonian Basin (Kováč and Hók, 1996; Lexa and Konečný, 1998).

Tectonically, the Outer Carpathians correspond to the Tertiary accretionary complex related to the southward subduction of the oceanic to the sub-oceanic crust at the European Plate margin. From the Inner Carpathians, they are separated by the Pieniny Klippen Belt (PKB), commonly considered as a deep-seated boundary between the colliding European Plate and the microplate ALCAPA (McCann, 2008). The Pieniny Klippen Belt is assumed to be one of the surface expressions of the Late Cretaceous to Early Tertiary closure of the Penninic-related oceanic domain forming a boundary between the inner and outer units of the Carpathian orogen (Plašienka et al., 1997).

The Pieniny Klippen Belt as the boundary between the Outer Carpathians, overlying the subducted margin of the European Plate, and the Inner Carpathians of the ALCAPA microplate, is an important first-order tectonic structure in the Carpathians. It forms a 600-km long and a few kilometres wide zone of extreme shortening which extends along the Carpathian belt (McCann, 2008). The PKB is composed of several successions of mainly deep- and shallow-water limestones mostly of Jurassic to Cretaceous age and its sequences are submerging sub-vertically down to depths of at least 5 km (e.g., Bielik et al., 2004; Birkenmajer, 1986; Tomek, 1993; Vozár et al., 1998). Strong tectonic deformation is a result of two main phases during the Alpine orogeny. Its present surface structure can be explained as resulting from extensive and complex transpressional to transtensional movements that affected the originally shallow fold-and-thrust belt (Kováč and Hók, 1996; Němčok and Němčok, 1994). In most areas, the Pieniny Klippen Belt forms the axial part of a broad flower structure which also includes the innermost units of the Carpathian Flysch and the frontal units of the Inner Western Carpathians. Though there are attempts to interpret the sub-vertical structure of the Pieniny Klippen Belt to depths of about 12 km (Vozár et al., 1999), there is no seismic evidence about its continuation to the middle and lower crust (Hrušecký et al., 2006).

3. Existing velocity models

The crustal and upper-mantle velocity structure gives the basis for subsequent seismic studies of local features. In the Western Carpathians and their surrounding units, it was derived from seismic refraction experiments CELEBRATION 2000, ALP 2002, and SUDETES 2003 (Brückl et al., 2003; Grad et al., 2003a,b; Guterch et al., 2003) covering

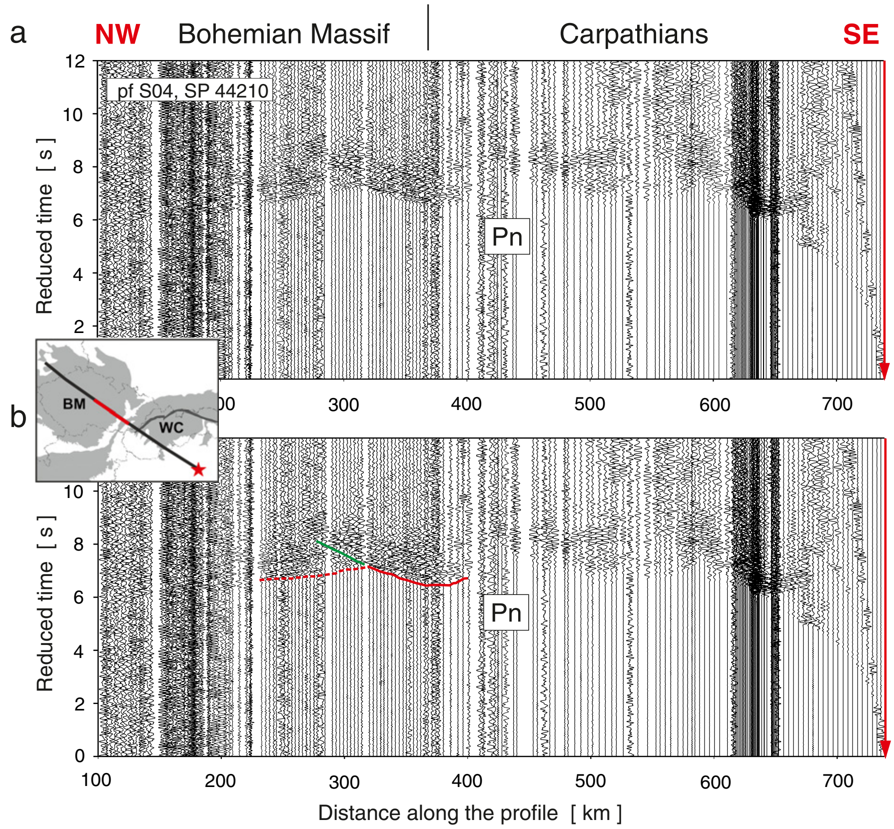

Fig. 2. Example of refraction and wide-angle reflection data with anomalous *Pn* phase. (a) Amplitude-normalized vertical component seismic section for the shot point SP 44210, profile S04 plotted with reduction velocity of 8 km/s. (b) The same seismic section with marked anomalous *Pn* phase. Note strong first-arrival *Pn* phase with low apparent velocity <8 km/s (solid red line). Green line represents continuation of this *Pn* phase to later arrivals determining the abrupt change of the Moho topography. Note the shape of the *Pn* phase and its continuation to later arrivals resulting in the complex local Moho topography.

mainly the Czech Republic, Slovakia, Poland, Hungary, and Austria. Data from these experiments were interpreted by standard tomographic and trial-and-error forward modelling of the refracted and reflected seismic phases resulting in 2D or 3D velocity models. These models indicate that the thickness of the crust across the Western Carpathians changes from 25 to 30 km beneath the Pannonian Basin in the south, to 35–43 km close to their axial part (PKB) and reaches 30–45 km in their northern foreland (Grad et al., 2006; Hrubcová et al., 2010; Środa et al., 2006). In the north, a Moho depression was interpreted which seems to be confined to the central part of the Western Carpathians as it was observed in the CEL01, CEL04, and CEL05 profiles (Grad et al., 2006; Środa et al., 2006; Środa, 2010). In the west, the Moho depth in the Bohemian Massif ranges among 30–39 km with its maximum in central part of the Bohemian Massif (Hrubcová et al., 2005). At the contact of the Western Carpathians with the Bohemian Massif a sharp change of the Moho topography close to the contact of the PKB was interpreted from the S04 profile (Hrubcová et al., 2010).

Knowledge of a shallow structure is essential for proper modelling of deeper parts and its effect must be separated from modelled phases. The upper crust with sedimentary successions of the Carpathian Flysch and Foredeep shows pronounced lateral variations of seismic velocity, causing substantial differences in the travel times of both crustal and upper mantle phases emerging in this area. Considerably lower velocities of 3.8–4.2 km/s down to a depth of 7 km are detected in a distance range of 370–460 km along the profile S04 modelled also by Hrubcová et al. (2010); velocities in a range of 2.5–5.5 km/s down to a depth of 10 km are modelled along the profile CEL09 (Hrubcová et al., 2005). Similar velocity structure was detected also in the northern rim of the Western Carpathians along profiles CEL04 (Środa et al., 2006) and CEL05 (Grad et al., 2006). Such velocities correspond to the Tertiary sediments of the Outer Western Carpathians: the Carpathian Flysch and the Carpathian Foredeep. The thickness of sediments of the Carpathian Flysch is also constrained by the reflection profile 8HR (Tomek and Hall, 1993) and by geological information (e.g., Golonka and Krobicki, 2004; Vozár et al., 1999). Very low velocities of ~2.2 km/s to a depth of 0.5 km at a distance of 425 km along the CEL09 profile reflect the Neogene to Quaternary sediments of the Alpine Molasse Vienna Basin margin (Hrubcová et al., 2005).

4. Anomalous *Pn* phases

The anomalous upper-mantle *Pn* phases used for the interpretation were identified in seismic sections from all three experiments CELEBRATION 2000, ALP 2002, and SUDETES 2003. The western part of the Western Carpathians at the contact with the Bohemian Massif is interpreted from data along profiles CEL09, CEL15 (CELEBRATION 2000 experiment), ALP01 (ALP 2002 experiment), and S04 (SUDETES 2003 experiment). The northern rim of the Western Carpathians, at the contact with the North and East European Platforms, is documented from profiles CEL01, CEL04, CEL05, and CEL11 (CELEBRATION 2000 experiment). The situation of profiles is presented in Fig. 1; details of data processing are described in Hrubcová et al. (2005) or Środa et al. (2006).

The seismic sections along all these profiles comprise *Pn* phases coming from the upper mantle with anomalously low (western parts) or high (northern parts) apparent velocities and of high amplitudes. These phases are identified in the first arrivals, often with a continuation to later arrivals, and are characterized by an abrupt change of the apparent velocity in contrast to a typical *Pn* phase with the velocity of ~8 km/s. This suggests complex local Moho topography.

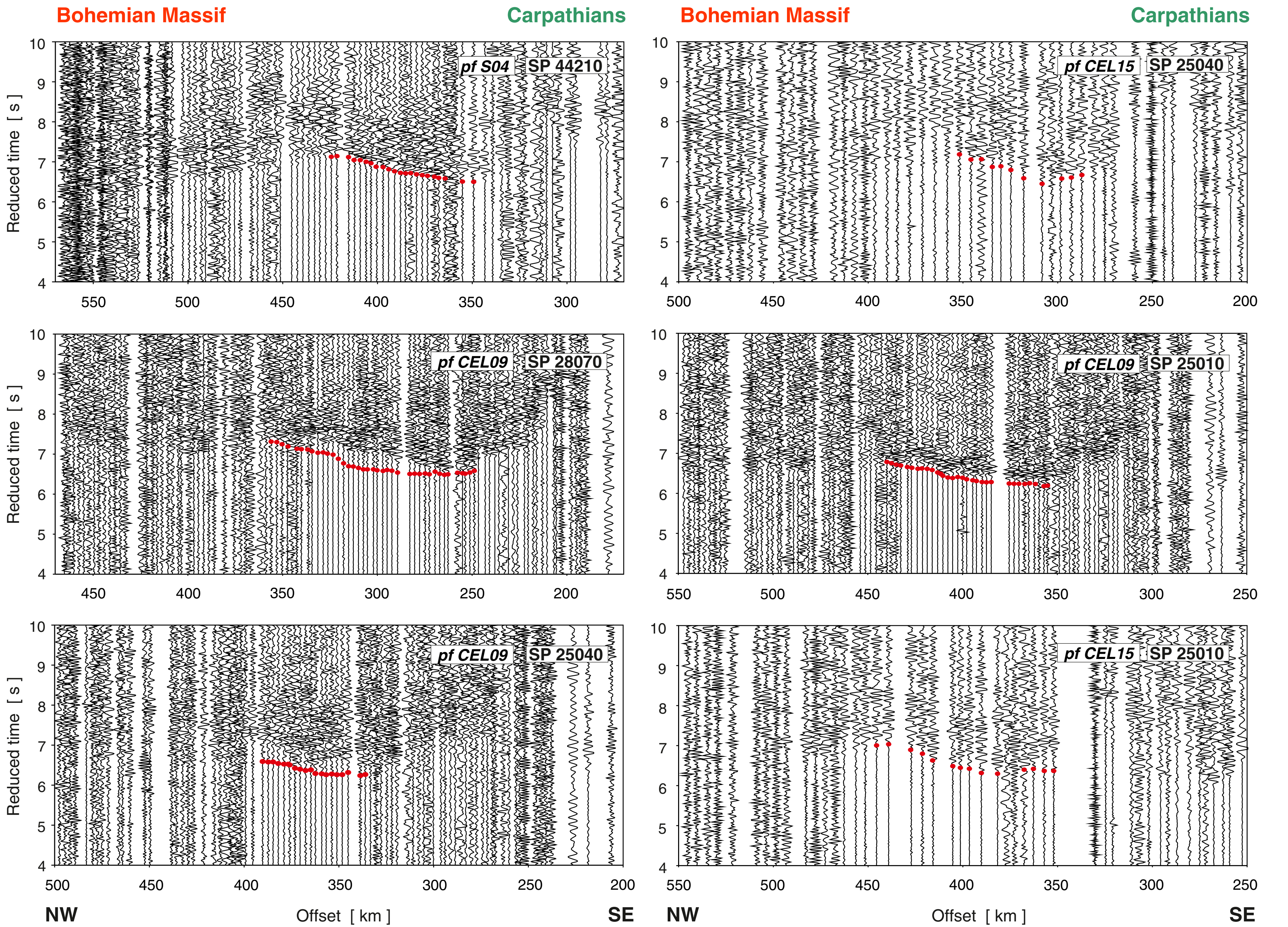

Fig. 3. Examples of amplitude-normalized vertical component seismic sections with anomalous *Pn* phases originating at the contact of the Bohemian Massif and the Western Carpathians with shot points in the Pannonian Basin. Seismic sections plotted with reduction velocity of 8 km/s and band-pass filtered from 2–15 Hz. Note strong seismic *Pn* phase and its continuation to later arrivals with low apparent velocity <8 km/s.

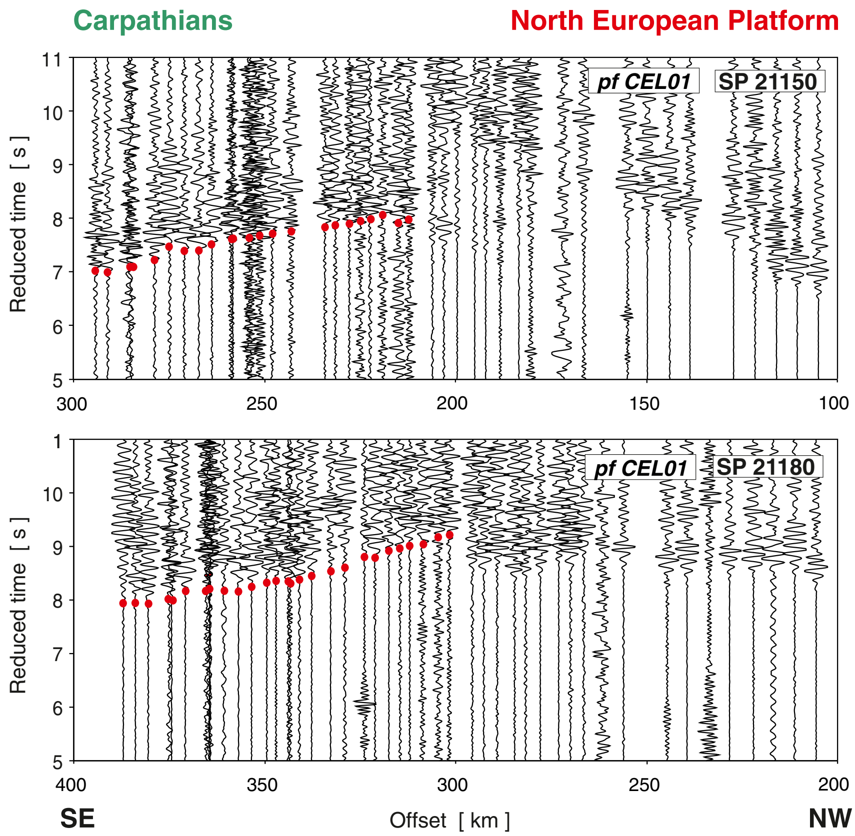

Fig. 4. Examples of amplitude-normalized vertical component seismic sections with the anomalous *Pn* phases originating at the contact of the Carpathians with the European Plate and the shot points in the north. Seismic sections plotted with reduction velocity of 8 km/s and band-pass filtered from 2–15 Hz. Note strong seismic *Pn* phase with high apparent velocity > 8 km/s.

In the west, the NW–SE oriented profiles CEL09 (length 740 km), CEL15 (length 530 km) and S04 (length 740 km) start at the northwestern edge of the Bohemian Massif, continue across the Western Carpathians, and terminate in the Pannonian Basin. The anomalous *Pn* phases are identified in seismic sections from both in-line and off-line shots mainly located in the SE in the Pannonian Basin. One seismic section from the off-line shot point located in the Pannonian Basin exhibits the anomalous *Pn* phases along the N–S oriented ALP01 profile (length 645 km). The distinctive *Pn* arrivals show low apparent velocity of about 7.3 km/s connected with a local increase of the amplitude. Furthermore, these strong low-velocity first arrivals often continue to later arrivals with higher amplitude than the preceding *Pn* phase (Fig. 2). These phases do not represent an isolated phenomenon attributed to only one place or one seismic section; they are visible in 14 seismic sections both for the in-line and off-line shot points located in the southeast in the Pannonian Basin and recorded in the northwest direction (Fig. 3). Though they are observed at various offsets from the shot points (from 180 to 400 km), they are always located at a similar distance from the Western Carpathian axis. This suggests that they originate close to the contact of the Western Carpathians with the western units, the Bohemian Massif.

The profiles crossing the northern rim of the Western Carpathians, the CEL01 (length 880 km), CEL05 (length 1420 km) and CEL11 (length 430 km) are of the NNE–SSW direction; the profile CEL04 (length 630 km) is of the NNW–SSE direction. Here, strong upper-mantle arrivals show abnormally high apparent velocity (~9 km/s or more) observed for rays crossing the Carpathian orogen from the north at a similar distance from the Pieniny Klippen Belt (recorded at distances of ~0–150 km from PKB). The amplitude of these phases is higher or at least equal to the typical *Pn* amplitude and these phases are clearly visible even if the typical *Pn* phase is not observed at all. These phases are observed in seismic sections of 43 in-line and off-line shot points mostly located north of the Carpathians (Fig. 4). Środa (2010) suggested that they represent anomalous *Pn* or diffraction-like arrivals produced by small, local anomalies of the Moho topography close to the Pieniny Klippen Belt.

The distinctive *Pn* arrivals in the west and north of the Western Carpathians differ in terms of the apparent velocities visible in seismic sections. In the western part of the Western Carpathians, these phases are visible in sections from the shot points in the southeast and show low apparent velocities; in the northern parts they are visible for the shot points located north of the Western Carpathians with high apparent velocities. The detected apparent velocities differ due to different position of shot points in respect to tectonic plates. Low apparent velocities are observed in seismic sections with shots in the over-thrusting ALCAPA microplate; high apparent velocities occur in seismic sections with shots in the stable subsiding European Plate. However, independently of different apparent velocities and of different propagation directions, modelling suggests that the origin of these phases seems to be similarly confined to a relatively narrow anomaly associated with localized structures at the Moho boundary close to the axis of the Carpathian orogen.

5. Modelling of the anomalous *Pn* phases

The topography of the Moho in seismic refraction modelling is inferred from the wide angle reflected *PmP* phases complemented the refracted uppermost mantle *Pn* phases. In tectonic areas, especially when the local Moho topography is complicated, the *PmP* phases are not always distinguished in the recorded seismic sections and the refracted *Pn* phases serve as the main source for modelling. In the Western Carpathians, at their contact with surrounding tectonic units, complex Moho geometry and strong attenuation in the deformed crust does not allow for clear observations of the Moho *PmP* reflections.

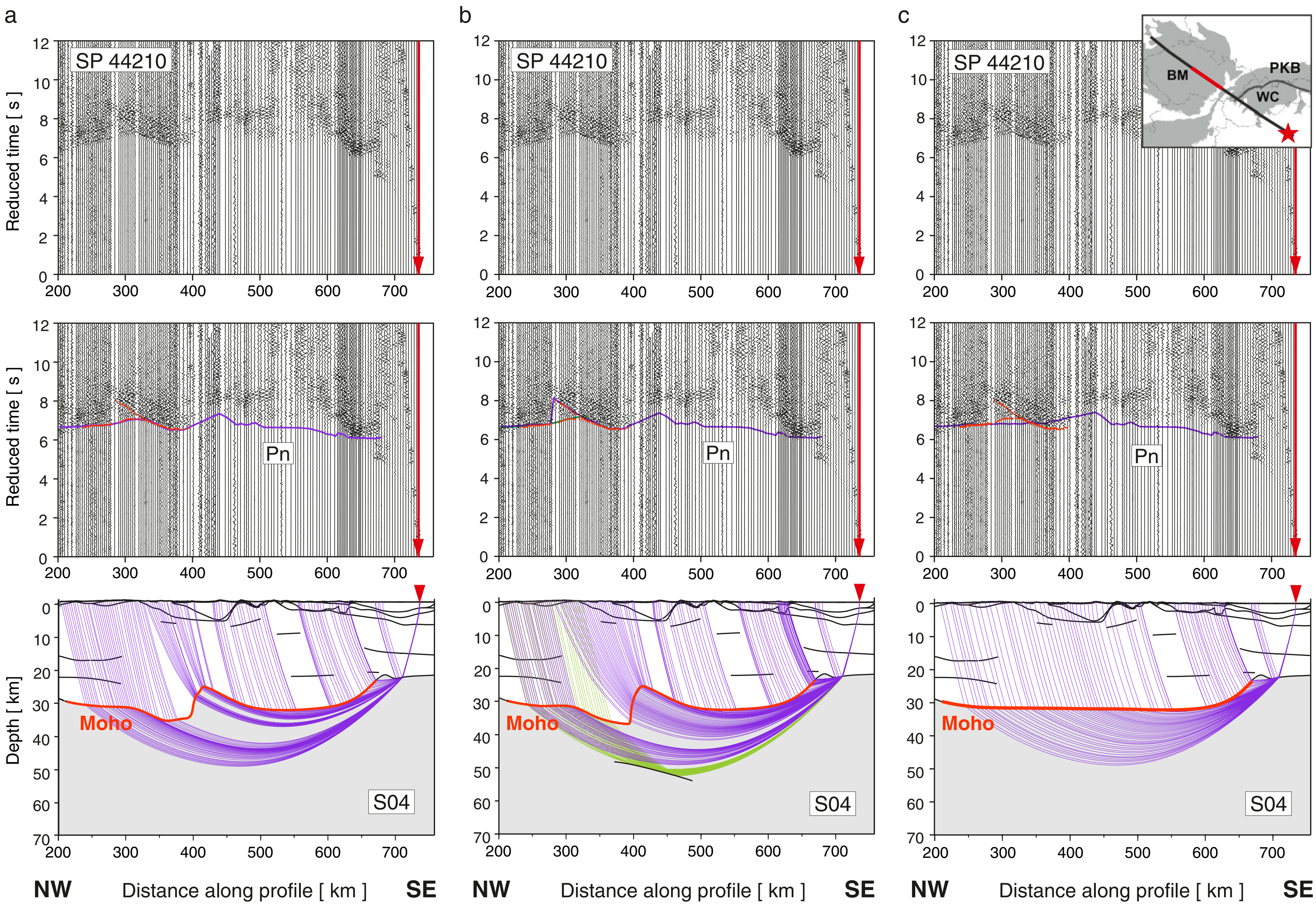

Fig. 5. Forward modelling with ray tracing along the S04 profile (SP 44210) documenting the Moho shape at the transition between the Western Carpathians (WC) and the Bohemian Massif (BM). (a) Effect of a dipping Moho modelled with only the first *Pn* arrivals; (b) effect of a steeply dipping Moho modelled also with picks in later arrivals (after Hrubcová et al., 2010), weaker preceding arrivals modelled with local upper-mantle reflector; (c) effect of a flat Moho. For each part of the figure: top — amplitude normalized record sections; middle — amplitude normalized record sections with theoretical travel times; bottom — models and ray paths. Violet lines mark *Pn* refraction from the upper mantle, green line represents upper-mantle reflection; red dots mark the interpreted data (picks) both in the first and later arrivals. Black lines mark model discontinuities constrained by reflections and interfaces in the uppermost crust well-constrained by refractions. Data have been band-pass filtered from 2–15 Hz; reduction velocity is 8 km/s. Note good fit for the *Pn* and/or strong later arrivals with picks in case of the dipping Moho (a,b) compared to a missing response for picks in case of a flat Moho (c). Note also the *Pn* refraction in the first and later arrivals controlling the shape of the Moho topography.

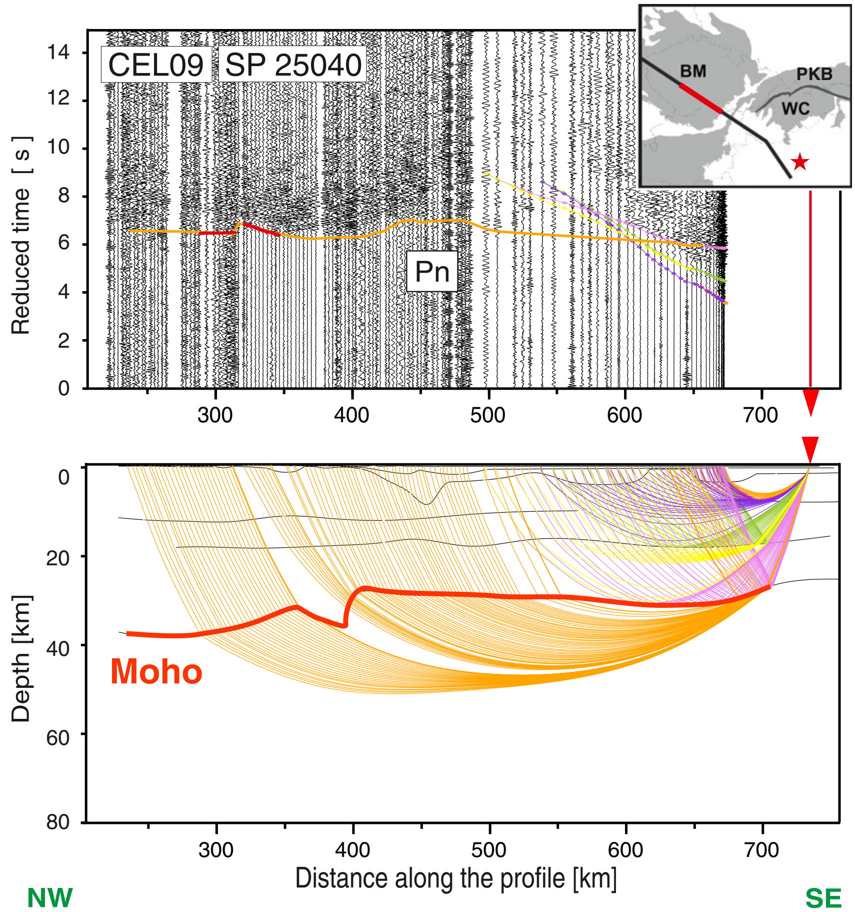

Fig. 6. Forward modelling with ray tracing documenting the Moho at the transition of the Carpathians (WC) with the Bohemian Massif (BM) along the CEL09 profile (SP 25040). Top — amplitude normalized record section with theoretical travel times (*Pn* refraction from upper mantle marked in yellow), red dots mark the interpreted data (picks); bottom — model and ray paths. Data have been band-pass filtered from 2–15 Hz; reduction velocity is 8 km/s. PKB, Pieniny Klippen Belt. Note the shape of the anomalous *Pn* phase and its continuation to later arrivals resulting in the complex local Moho topography.

Instead, the anomalous *Pn* phases are identified in the seismic wavefields. Thus, in our approach, the Moho is constrained by the *Pn* phases. However, strong amplitudes of the *Pn* phases give a solid basis for the interpretation of the Moho topography.

To model the upper-mantle *Pn* phases, we applied forward iterative travel time fitting using the ray-tracing program package *SEIS83* (Červený and Pšenčík, 1984) supplemented by an interactive graphical interface *MODEL* (Komminaho, 1997) and *ZPLOT* (Zelt, 1994). The modelling involved calculation of travel times; synthetic sections helped to constrain the velocity contrasts and the shape of the Moho and generally showed good qualitative agreement with the relative amplitudes of the observed phases.

Modelling of the *Pn* phases is based on the existing velocity models of crust and upper-mantle, where also complicated shallow structure is taken into account. These models explain a large part of the observed wavefields and allow isolating the anomalies of the *Pn* phases close to the contact with the Carpathians. Modelling of these phases enabled to focus on local changes of the Moho topography.

5.1. Western side of the Carpathians

Modelling of the Moho structure at the western side of the Western Carpathians at their contact with the Bohemian Massif was performed with data from the profiles S04, CEL09, CEL15 and ALP1. For profile S04, the seismic section from the shot point SP 44210 in the Pannonian Basin shows the *Pn* phase with the apparent velocity of 7.3 km/s observed in the first arrivals in a distance range of 320–390 km, which continues to later arrivals up to a distance of 270 km. Based on the velocity model of Hrubcová et al. (2010), modelling of the anomalously low velocity *Pn* phase results in a NW-dipping Moho at a distance of 390–415 km with ~12 km change of the crustal thickness from 25 to 37 km. The shape of the Moho topography is constrained from shot points SP 44210, 44140, and 44100. Fig. 5 shows the effect of the Moho topography in data from seismic section for SP 44210. It compares the effect of steeply dipping step-like Moho with response from a model with a flat Moho. In the case of the step-like Moho anomaly, the fit for the *Pn* phase is achieved for the first arrivals (Fig. 5a) and for both the first and later arrivals (Fig. 5b). In both cases, the fit results in slightly different shape of the Moho topography where later *Pn* arrivals control the bending shape of the step. In case of the situation in Fig. 5b, the fit is achieved in combination with a local upper mantle reflector at a distance of 370–460 km and a depth of ~50 km situated beneath the Moho depth anomaly. In these examples, the shape of the Moho topography slightly differs, nevertheless, the location of the anomaly along the profile remains at the same place for both cases. On the other hand, Fig. 5c shows the situation where the fit is missing for a flat Moho.

In case of the S04 profile, where later *Pn* phases are clearly detected, the favourable model is presented in Fig. 5b. Here, the later arrivals are modelled as the *Pn* refraction resulting from the steep inclination of the step. The weaker preceding arrivals visible in seismic sections are interpreted as reflection from the mantle and modelled with local upper-mantle reflector close to the Moho anomaly. Nevertheless, not all modelled sections with anomalous apparent velocities show continuation of the *Pn* phase to later arrivals. Thus, the comparison of Fig. 5a

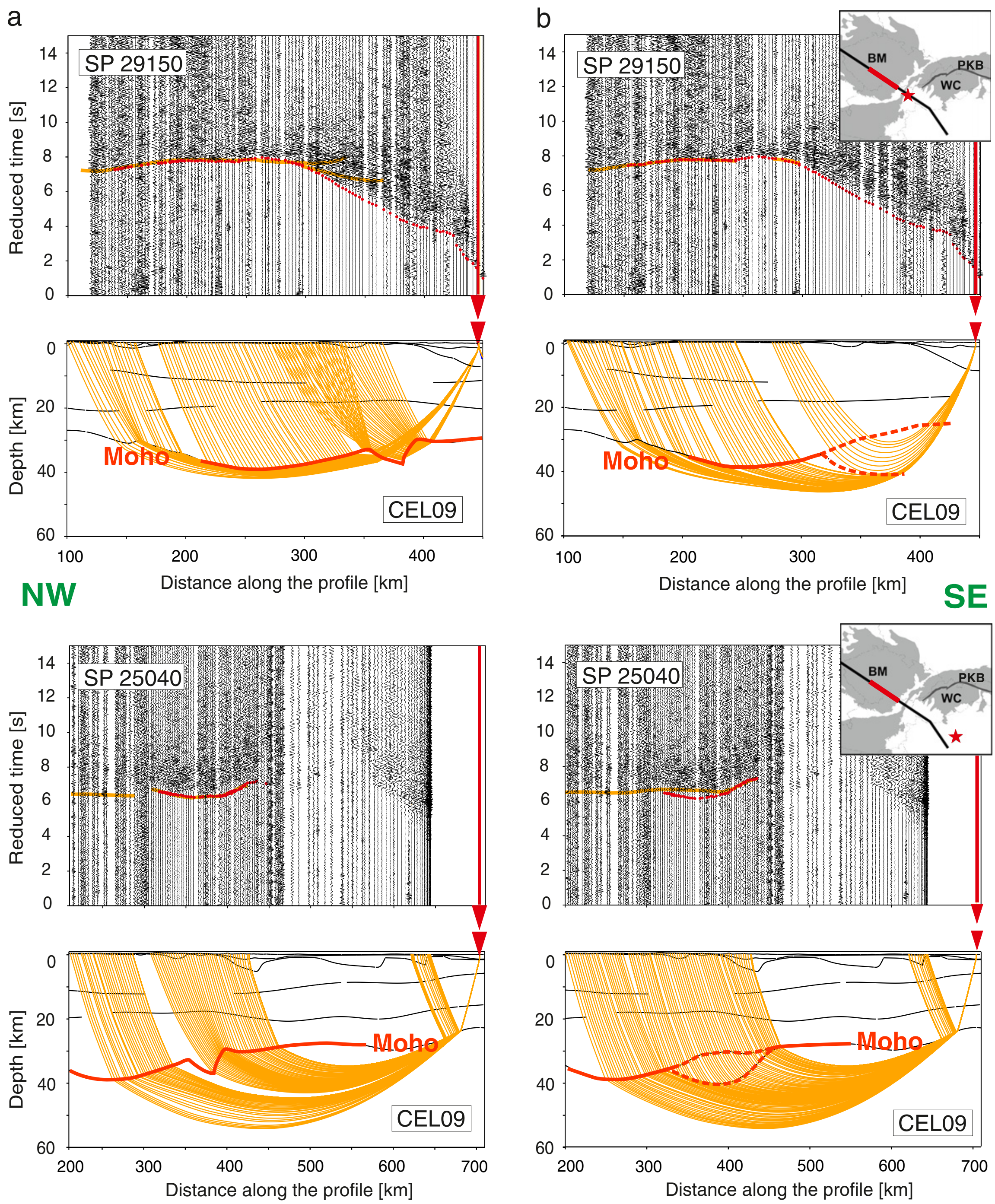

Fig. 7. Modelling of different crust-mantle transition along CEL09 profile illustrating possible solutions at the contact of the Carpathians (WC) with the Bohemian Massif (BM). Forward modelling with ray tracing for shot points SP 29150 (in the Carpathian Flysch) and SP 25040 (in the Pannonian Basin). (a) Velocity contrast at the Moho with the Moho anomaly as in Fig. 6. (b) Gradient crust–mantle transition zone as according to Hrubcová et al. (2005). For each part of the figure: top – amplitude normalized record sections with calculated travel times (yellow lines) and data *Pn* picks (red dots); bottom – models and ray paths. Moho topography (red solid lines) and gradient lower crust (red dashed lines) highlighted. Data have been band-pass filtered from 2 to 15 Hz; reduction velocity is 8 km/s. Note that the calculated travel times for both interpretations of the SP 29150 satisfy the data. But for the SP 25040, the fit of the calculated travel times with the identified *Pn* arrivals is much better for the Moho anomaly (left panel) compared to missing fit in case of the gradient zone (right panel). PKB, Pieniny Klippen Belt.

and b illustrates the situation when later arrivals are observed or not and, to some extent, documents the ambiguity of the modelling with respect to the detected phase.

In a similar way, the shape of the Moho anomaly at the transition between the Bohemian Massif and the Carpathians is modelled by forward modelling of the seismic sections along other profiles, both for in-line and off-line shot points. All 14 seismic sections used for the interpretation have shot points located in the SE in the Pannonian Basin along profiles CEL09, CEL15, S04 and ALP01 and show distinct low-velocity *Pn* phase sometimes with continuation to later arrivals. The shape of the Moho modelled along the CEL09 profile located ~80 km to the south of profile S04 is presented in Fig. 6. There, the velocity modelling of Hrubcová et al. (2005), who modelled the Bohemian Massif up to its contact with the Carpathians, is extended for two in-line shot points SPs 21031 and 25040 in the Pannonian Basin where crossing profiles CEL01 and CEL05 (Grad et al., 2006; Środa et al., 2006) help to constrain local structure in the Pannonian Basin beneath these shot points. New velocity model along extended

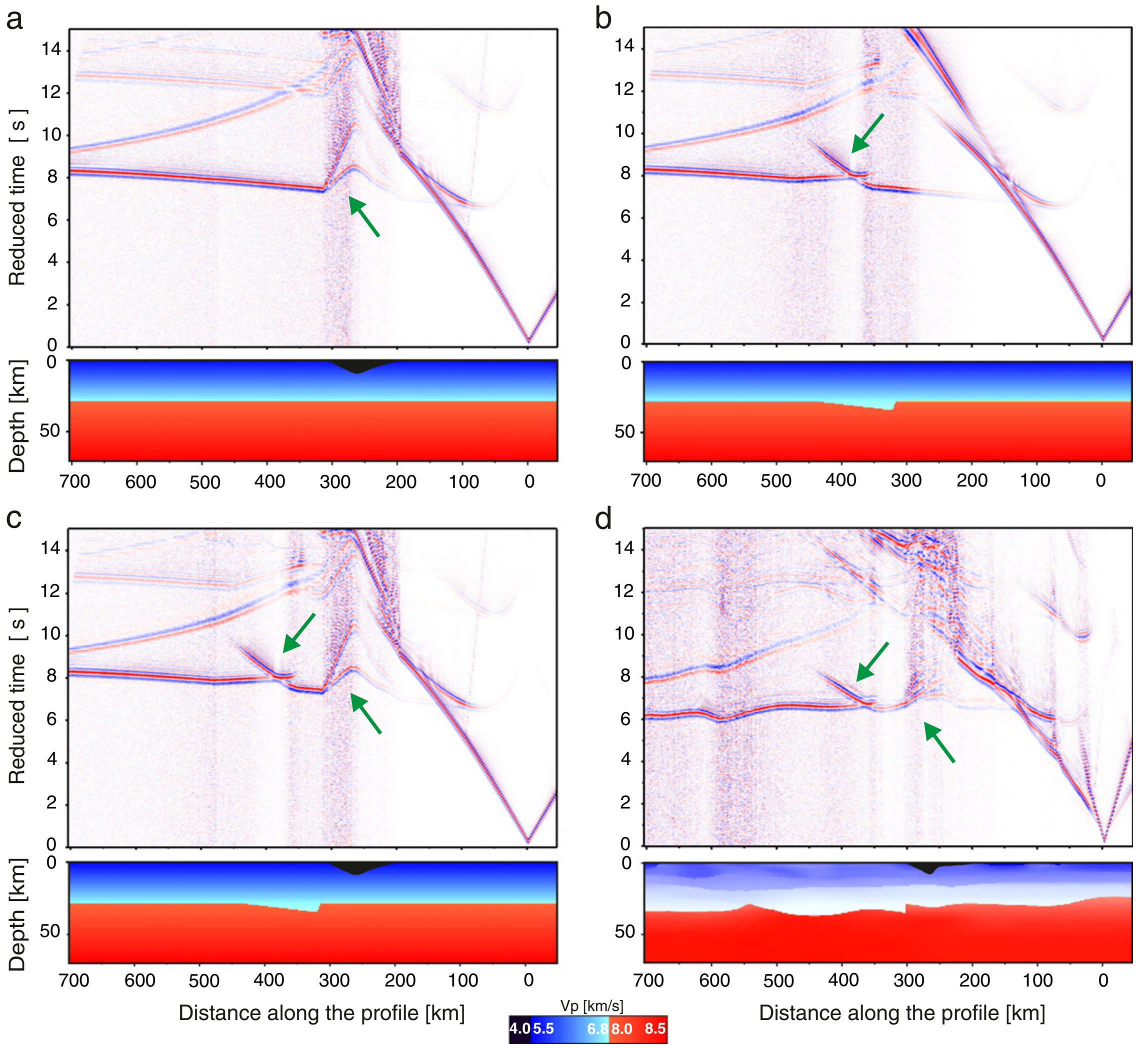

Fig. 8. Full waveform synthetic tests calculated with finite difference code MPM (Hansen and Jacobsen, 2002). Documentation of the origin of phases close to the contact of the Western Carpathians with the Bohemian Massif. (a) Effect of a low velocity Carpathian Flysch; (b) effect of an abrupt change of the Moho topography modelled with steeply dipping Moho; (c) combination of both effects; (d) both effects in real velocity model S04 derived from ray tracing. For each part of the figure: top — synthetic sections with time reduced to 8 km/s; bottom — *P*-wave velocity model. Green arrows mark the effects in the data. Crustal velocity marked by shades of blue; upper-mantle velocities marked by red; black colour marks sediments of the Carpathian Flysch.

CEL09 profile is constrained from SPs 29140, 29150, 21031 and 25040, and suggests a depth change of the Moho topography to the NW from 28 to 35 km at a distance of about 380 km along CEL09 profile, close to the contact of the Western Carpathians with the Bohemian Massif.

Previously, Hrubcová et al. (2005) modelled the crustal structure of the Bohemian Massif up to its contact with the Carpathians along NW part of the CEL09 profile. Beneath the Moravo-Silesian in the Brunovistulian unit, i.e., NW of the Carpathians, the Moho reflections were not observed. Especially, the section SP 29150 at a distance of 450 km along the CEL09 profile exhibited quite unusual character where only the first arrivals were identified as a strong *Pg* phase turning into a very strong *Pn*. Apart from this, a weak phase with a high apparent velocity was identified beyond the bending point of the first arrivals in place where the *Pg* turned into the *Pn* phase. Hrubcová et al. (2005) interpreted such a shape of travel times with a vertical gradient increase without velocity discontinuities. Instead of a sharp Moho, they proposed a 17 km thick gradient zone at depths of 23–40 km with *Vp* velocities ranging from 6.8 to 7.8 km/s as a characteristic feature of the Brunovistulian unit. Since Hrubcová et al. (2005) concentrated on the Bohemian Massif, their interpretation did not go beyond the contact with the Carpathians. However, extending the modelling for seismic sections in the Pannonian Basin that we do in this study allows for a wider range of possible solutions. Fig. 7 illustrates two possible interpretations of the crust–mantle transition from the shot point SP 29150 in the Carpathian Foredeep and the SP 25040 in the Pannonian Basin. It compares the *Pn* for the first-order Moho discontinuity with the step-like Moho anomaly (Fig. 7a) and the gradient crust–mantle transition zone as according to Hrubcová et al. (2005) (Fig. 7b). Since the SP 29150 is quite close to the Moho anomaly, its section cannot exhibit the anomalous *Pn* phases. Nevertheless, Fig. 7a documents that the SP 29150 section can be interpreted with the Moho step as well as with the gradient zone. From the calculated travel times it is clear that both interpretations for the SP 29150 satisfy the data. Similar situation is for the reciprocal shot points, e.g., SP 29060 (located in the Bohemian Massif), which allow both interpretations. To decide which solution is preferable, we have to look at the sections in the Pannonian Basin with the anomalous *Pn* phases. Section SP 25040 shows that the fit of the calculated travel times with the identified *Pn* arrivals is much better for the step-like Moho anomaly compared to missing fit in case of the gradient zone (Fig. 7b). Thus, although the usual approach is to try to reach an agreement with previously published results, in this case we suggest the first-order Moho discontinuity with the Moho topography change as a more probable solution at the contact with the Bohemian Massif. Nevertheless, this is a complicated tectonic area and a combination of the effect of a gradient zone at the Moho

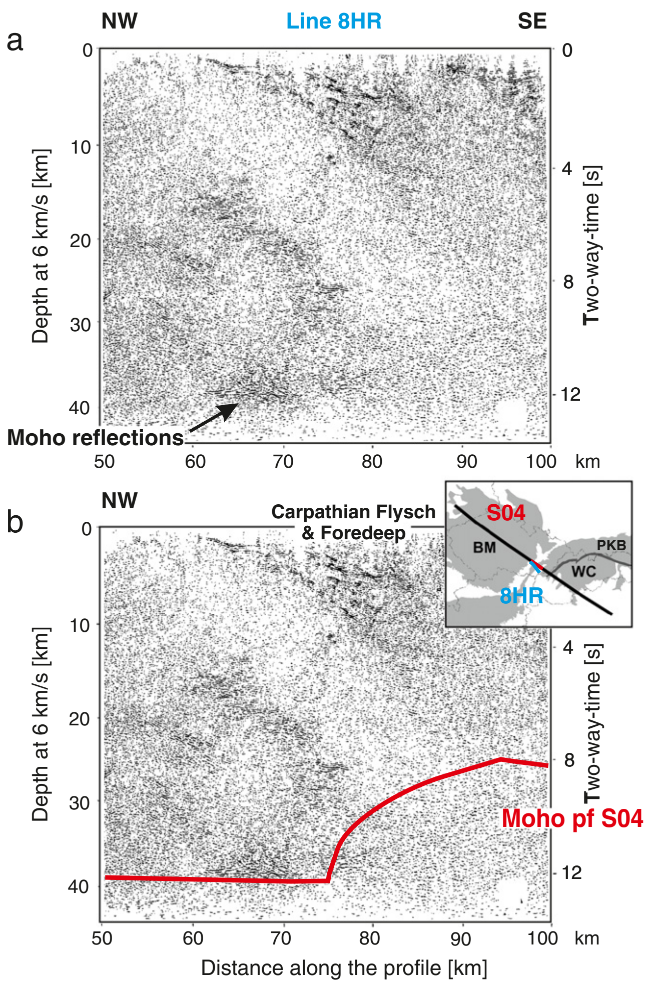

Fig. 9. Reflection profile 8HR at the contact of the Western Carpathians with the Bohemian Massif. (a) Part of the migrated reflection profile 8HR in scale 1:1 (after Tomek and Hall, 1993). (b) The Moho topography modelled along the S04 profile (red line) superimposed on top of the 8HR profile. Inset marks locations of 8HR and S04 profiles. Note well-defined sub-horizontal reflections at a distance of 60–75 km, depth of 38 km, interpreted by Tomek and Hall (1993) as the Moho reflection of the Bohemian Massif. They fade out at ~77 km distance, close to the projected location of the S04 Moho step. Similarly, strong lower crustal reflectivity at 20–38 km depth, visible up to a distance of 70–75 km does not continue beyond the location of the S04 Moho depth change. Spatial coincidence of both features suggests their common origin.

level (proposed also by Hrubcová et al., 2008) next to a sharply pronounced Moho with a step can represent the complexity of the area as was also discussed by Hrubcová et al. (2010) along the profile CEL10.

The modelling along the extended profile CEL09 also involves seismic sections located slightly off the CEL09 line (SP 27020, 27030, 27050, 27060, 27070, 28070, 28080 and 28090). Since these shot points are not located at the CEL09 profile directly, the upper crustal parts near the shot points were taken from the velocity models along the profiles CEL07 and CEL08 (Malinowski and CELEBRATION 2000 Working Group, 2003) to avoid the influence of the local upper crustal conditions on the interpreted mantle phases. Results of the forward modelling show a change of the Moho topography from 28 to 38 km at a distance of 380 km along the CEL09 profile. Since the geometry for the off-line modelling is not exactly 2D, the actual position of the modelled Moho anomaly in this case is off the CEL09 line, slightly more to the south. In a similar way, the seismic section of the off-line shot point SP 37070 with anomalous upper-mantle phases recorded along the ALP01 profile can be used. Such interpretation can give an indication of the location of the Moho anomaly more to the south of the CEl09 profile, though in this case the use of velocity model along the CEL09 profile would be more approximate and the precision of determination the Moho structure would be lower. For this reason, we did not include this modelling into our final results.

Similar shape of the Moho anomaly is also achieved from data along the profile CEL15 located close to the S04 line. The seismic section from the off-line shot point SP 25040, which is located at the prolongation of the CEL15 line along the S04 line, also exhibits the anomalous *Pn* phases. The CEL15 profile runs almost parallel with the S04 profile, and terminates at a distance of 530 km along the S04. For modelling of the seismic section from SP 25040, we combine the CEL15 velocity model with the model along the S04 line (Hrubcová et al., 2010) with the aim to concentrate on the Moho topography at the Western Carpathian contact. The step-like Moho anomaly bending to the NW is modelled at a distance of 400–420 km along the CEL15 with a depth change from 26 to 35 km.

5.2. Northern side of the Carpathians

The northern side of the Western Carpathians was studied from profiles CEL01, CEL04, CEL 05, and CEL11 of the CELEBRATION 2000 experiment (Grad et al., 2006; Janik et al., 2009; Środa et al., 2006), which covered the contact between the European Plate (East European Platform, Małopolska Block and Brunosilesian Unit) in the north, and the ALCAPA plate in the south. Some of the results of the refraction modelling revealed an abrupt change of the Moho depth from 35 km to 45 km forming local Moho depression with a width of ~15 km in the proximity of the PKB. The Moho anomaly at the northern rim of the Carpathians is different compared to the western parts. The Moho there is characterized by a local change of the Moho topography with similar depth on both sides forming a trough-like structure.

The anomalous upper-mantle phases at the northern rim of the Western Carpathians were interpreted by Środa (2010), who analysed them along profiles CEL01, CEL04, CEL05, and CEL11 and detected high amplitude mantle arrivals of unusually high apparent velocity (~9 km/s and more). These phases were generated by shots located north of the Carpathians (Małopolska Block and East European Platform) and recorded by stations in the Inner Carpathians. These phases, visible at large offsets (200–400 km), were quite pronounced and their amplitude was usually higher than the typical *Pn* amplitude (see Fig. 4). These arrivals were observed at a similar distance from the PKB (0–150 km to the south), which suggested that they originate in a local structure in the uppermost mantle beneath the Outer and Inner Carpathians. Środa (2010) suggested two alternative explanations of these phases: reflections from a north-declined discontinuity in the uppermost mantle, or arrivals generated by a localized anomaly at the Moho level (see Fig. 11d,e), acting similarly as a diffractor and turning up the *Pn* waves propagating in the mantle back to the surface. Such a localized anomaly could represent a relatively small fragment of the crustal material submerged in the mantle immediately below the Moho discontinuity with the velocity Vp of ~6.8 km/s forming a trough in a size of ~5–20 times ~5–15 km. However, Środa (2010) noted that the modelled rectangular geometry of the anomaly was just one of many possible solutions (including, e.g., irregularly shaped body) because the method used in his study allowed estimating mainly the size of the anomaly. Nevertheless, such an anomaly at the Moho level is analogous to the results of modelling along the profile V/3K (Uchman, 1975) where similar but wider Moho trough was also observed. Also, it coincides with the results from refraction modelling along profile CEL04 (Środa et al., 2006).

Compared to Środa (2010), local upper-mantle reflector close to the Moho anomaly was also interpreted by Hrubcová et al. (2010) who modelled local mantle reflector at a depth of 50 km at the western side of the Western Carpathians at the contact with the Bohemian Massif. Both in case of Środa (2010) and Hrubcová et al. (2010), local upper-mantle reflector is confined to the same place beneath the Moho depth change. Thus, the Moho anomaly and localized upper-mantle reflector may be connected and together they may reflect the

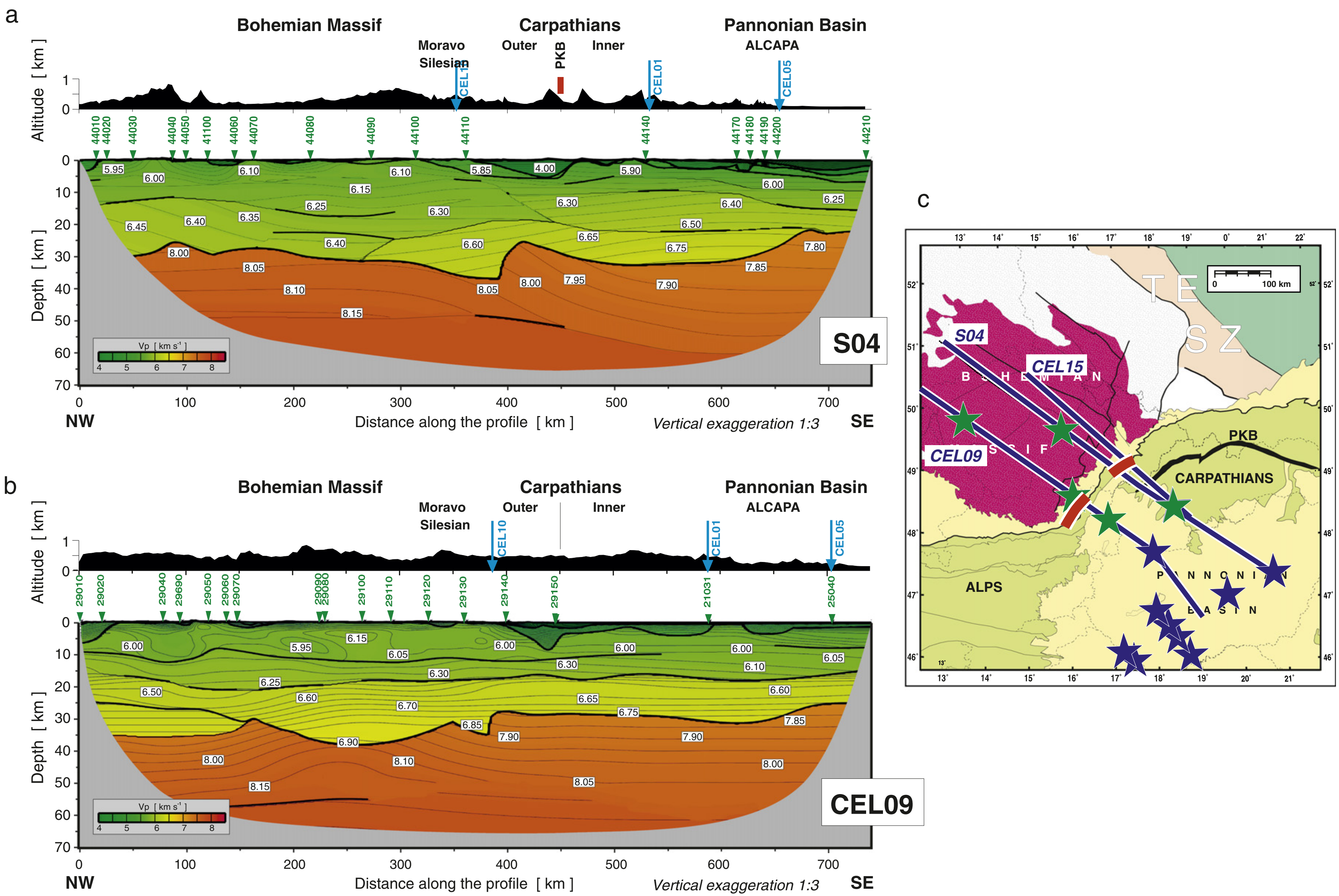

Fig. 10. *P*-wave velocity models derived from ray tracing at the contact of the Western Carpathians with the Bohemian Massif documenting the step-like Moho anomaly. (a) Model along profile S04 in scale 3:1. (b) Model along extended profile CEL09 in scale 3:1. (c) Situation of interpreted profiles and shots superimposed on tectonic map. Shots with anomalous *Pn* phases marked in blue; shots used for interpretation and constraints marked in green. Note Moho anomaly location derived from interpreted profiles (marked in red) and the position of the PKB (black).

complexity of structure at the contact of the Western Carpathians with the surrounding units.

6. Synthetic tests with full-waveform modelling

We performed synthetic tests to reduce misinterpretation of phases and to separate the effect of the upper crustal parts and deeper Moho topography. We tested for an effect of two structures: i) low velocities sediments of the Carpathian Flysch and Foredeep and ii) an abrupt change of the Moho topography. This approach enabled to document the origin of the anomalous phases, analyse individual phases in the recorded wavefields and verify the models from the ray tracing.

We applied finite-difference full-waveform modelling code of Hansen and Jacobsen (2002), as the fast and efficient tool for calculation of the full wavefield. The code uses fourth-order space and second-order time finite-difference solver of the elastic wave equation. The model was defined in terms of the *P*-wave velocities; *S*-wave velocity distribution was obtained from constant *Vp*/*Vs* ratio of 1.73. The velocity and density models were parameterized on a 2-D grid with 200 m spacing; the dominant frequency of the calculated wavefield was 4 Hz. Random noise with the same amplitude for all traces was added to the calculated seismograms to simulate realistic decrease of the signal-to-noise ratio with offset.

Full waveform results are summarized in Fig. 8. This figure presents a response from the model with complicated shallow structure represented by the low velocity Carpathian Flysch and Foredeep (Fig. 8a), a response from the abrupt change of the Moho topography modelled with steeply dipping Moho (Fig. 8b), and a response from the model with combination of these two structures (Fig. 8c). Fig. 8d presents a full waveform response of both effects in the realistic velocity model along the S04 profile derived from the ray tracing.

The models show that the thinning of the Carpathian Flysch and Foredeep in the SE direction increases the apparent velocity (8.7 km/s) in offsets closer to the shot points (offsets of 250–300 km), while lower apparent velocity (<8 km/s) at larger offsets (offsets of 350–400 km) results from the delay introduced by the Moho step. Thus, the variations in the upper crustal structure influence the apparent velocity of the *Pn* phase only at offsets of about 250–300 km. At larger offsets, the low-velocity Flysch and Foredeep sediments thin out completely and anomalies observed in this area originate from deeper crust or more likely at the Moho level.

7. Analysis of uncertainty

In wide-angle refraction modelling, errors of the resultant models come from a combination of several factors: data timing errors, travel

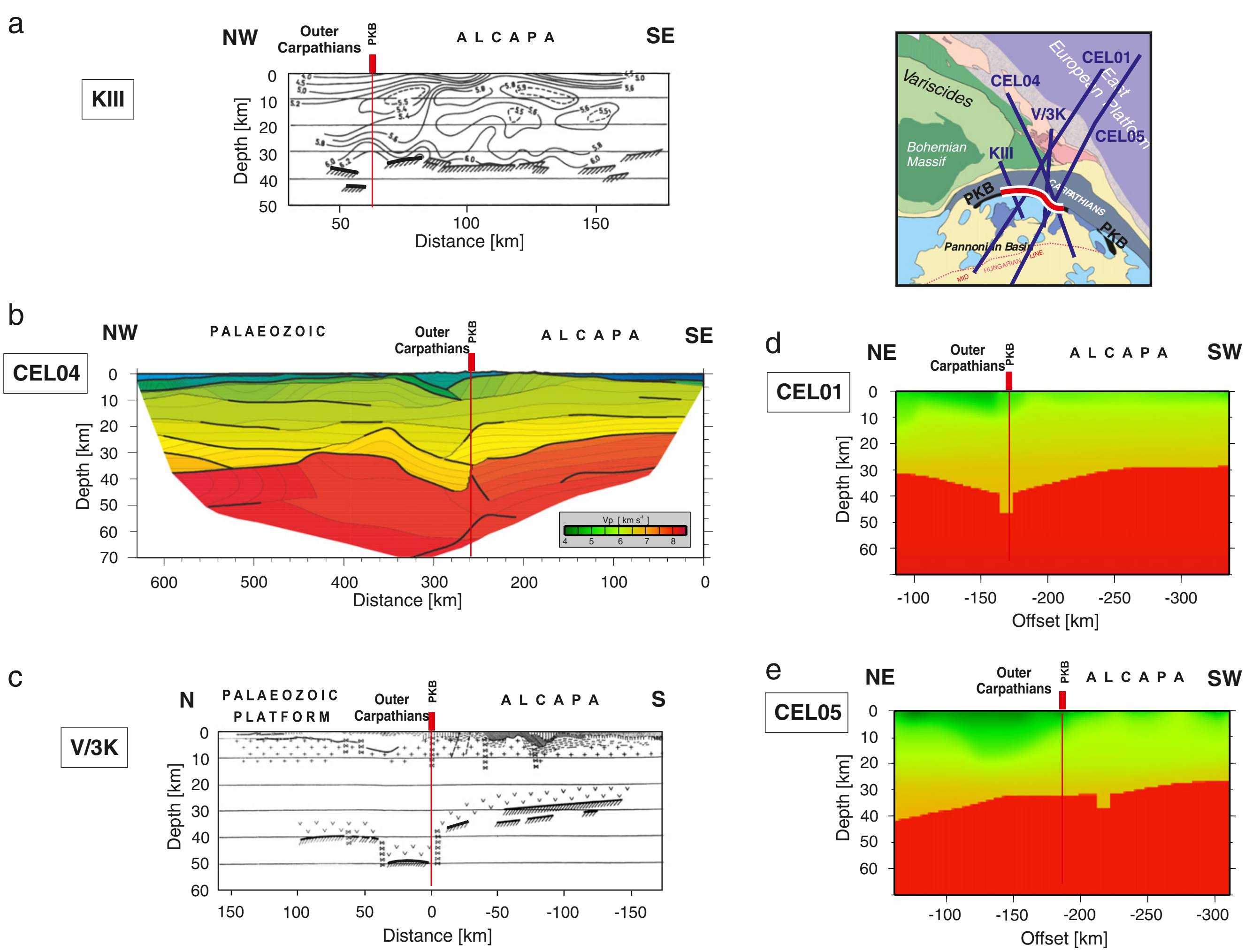

Fig. 11. Published velocity models with the Moho anomaly along seismic profiles in the northern part of the Western Carpathians. (a) DSS model along profile KIII in scale 1:1 (modified after Beránek et al., 1979). (b) Model from ray tracing along profile CEL04 in scale 3:1 (modified after Środa et al., 2006). (c) DSS model along profile V/3K in scale 2:1 (modified after Uchman, 1975). (d) Result of finite difference modelling along profile CEL01 in scale 2:1 (modified after Środa, 2010). (e) Result of finite difference modelling along profile CEL05 in scale 2:1 (modified after Środa, 2010). Inset shows the situation of profiles superimposed on tectonic map with projection of the Moho anomaly (marked in red). Note that though the models result from different seismic methods, they all show the Moho anomaly in the proximity of the PKB.

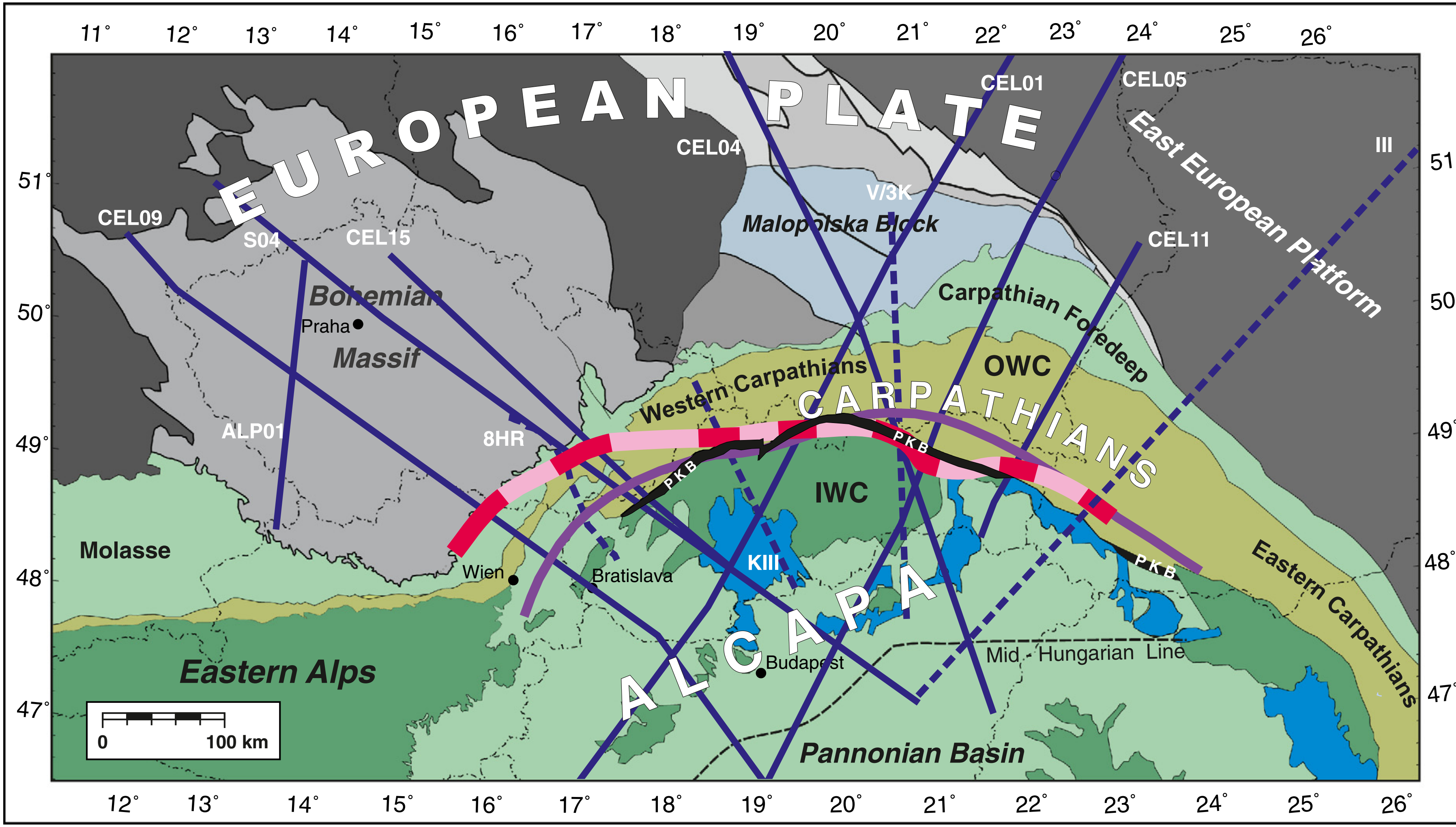

Fig. 12. Simplified tectonic map with projected Moho anomalies (red lines mark Moho anomalies detected at profiles; pink lines mark the interpolation between profiles) and projected axis of the Carpathian conductivity anomaly (magenta line, after Jankowski et al., 1985). Description of tectonic units as in Fig. 1a. Note the proximity of the Pieniny Klippen Belt (PKB) and both anomalies; note also varying position of anomalies along the Carpathian orogenic belt in respect to the PKB.

time picking and phase misidentification, inaccuracy of modelling (misfit between data and modelled travel times), isotropic approximation of a (potentially) anisotropic medium, and 2D method of interpretation not accounting for 3D structure. These factors and their limitations were discussed in Hrubcová et al. (2005, 2010).

According to that, realistic picking accuracy for the *Pn* phase is ~0.1–0.2 s. In case of typical wide-angle experiments with geometry allowing good ray coverage (with recordings from reciprocal directions) and modelling involving crustal/upper-mantle phases and Moho reflections, errors in determinations of the Moho depth is of the order of ~1–1.5 km. However, in this study there are several factors that can further influence the model accuracy. Thus, the analysis of uncertainty is more complex.

First of all, the Moho topography in the anomalous zone is not modelled from the *PmP* reflections, the most common phase for constraining the Moho. It is because the *PmP* phase in this part of the Carpathians is not observed or its amplitude is not high enough, so that it is not identified in the seismic sections with sufficient confidence. However, good quality *PmP* arrivals in the surrounding units in the north and west of the Carpathians allow for a robust modelling of the Moho depth beneath the Pannonian Basin or the Bohemian Massif and this serves as a reference for modelling in our study. Since the Moho geometry in the anomalous zone does not allow for clear observations of the *PmP* reflections and their detection in the seismic wavefields, the Moho topography is constrained by the *Pn* refractions from the uppermost mantle. These *Pn* phases and their continuations to later arrivals are correlated with the accuracy of ~0.2 s.

Even if the geometry of measurements enables recordings from reciprocal directions, the anomalous *Pn* phases are prevailingly available from shot points at one side of the profiles. This factor increases the ambiguity of the solution since the source of the modelled phases can be located in a 3-D volume as a result of side-reflected or diffracted energy. However, the anomalous arrivals cannot be interpreted by side-reflected waves propagating in the crust — in this case they would be observed at travel times later than crustal refracted waves. We do not observe this; the anomalous phases are part of the *Pn* phase, so that we interpret them as coming from the uppermost mantle. Also, we exclude the possibility of a crustal velocity anomaly reflecting/diffracting the emerging *Pn* phase — such an anomaly in the crust should influence the crustal phases as well, which we do not observed either.

Apart from the determination of the local Moho geometry, this study focuses also on positioning of the Moho anomaly relative to the axis of the Carpathian arc, i.e., its relation to the PKB. In this respect, we tested the uncertainty in the lateral position of the Moho anomaly. We calculated the response for modified S04 models where only the Moho step was shifted on both sides along the profile from the original location. These tests show that the lateral estimated uncertainty is ~15 km.

8. Comparison with other geophysical studies

8.1. Deep seismic soundings and reflection seismics

The first deep seismic models of the Western Carpathians were published by Uchman (1975) and Zátopek and Beránek (1975) along the N–S trending deep seismic sounding international profile V/3K located in Poland and Slovakia. Along this profile, they found an area with 50 km thick crust beneath the Outer Carpathians, separating the ~40 km thick crust of the North European Platform from thinner ~35 km crust of the ALCAPA beneath the Inner Carpathians. In the area of the thick crust, they modelled the Moho depression as a ~40 km wide trough, delimited by two sub-vertical fracture zones located beneath the PKB and to about 40 km north of it.

Regional seismic profile KII showed relatively deep and complex Moho with multiple reflectors over several kilometres depth to the west of the PKB compared to shallower, single Moho discontinuity to the east (Bucha and Blížkovský, 1994). Along the NW–SE profile KIII, the vertical Moho step of ~6–8 km was also modelled near the Pieniny Klippen Belt (Beránek et al., 1979). In the west, the deep seismic sounding along profile VI showed an abrupt change of the Moho depth at the contact with the Bohemian Massif (Beránek and Zátopek, 1981). In the east, the Moho step is also suggested along the profile III (Uchman, 1975).

The reflection profile 8HR crossed the contact of the Western Carpathians with the Bohemian Massif in the NW–SW direction. Tomek and Hall (1993) interpreted the reflection data from the 8HR profile as an image of the European continental crust obliquely subducted beneath the Carpathians. In the reflection section, the SE dipping and ~13 km thick unreflective area was interpreted as the upper crust of the European plate, relatively transparent compared to underlying highly reflective European lower crust and Moho. The upper edge of the subducting plate was imaged with a high curvature, but the Moho, imaged at ~38 km depth, showed sub-horizontal reflections strongest at a distance of 60–75 km along the 8HR line. However, further to the SE, the Moho reflections faded out at a distance of ~77 km. Similarly, strong lower crustal reflectivity, visible in a depth range of 25–38 km up to a distance of 60–77 km in the 8HR section, did not continue to SE.

The 8HR profile intersects at a very low angle the seismic refraction profile S04 close to the contact of the Carpathians with the Bohemian Massif. This intersection is near the place where the anomalous upper-mantle phases were interpreted (Fig. 9). Fig. 9a shows a part of the migrated time section of the 8HR profile between distances of 50 and 100 km (after Tomek and Hall, 1993); Fig. 9b displays the Moho topography modelled along the refraction profile S04 (Hrubcová et al., 2010) superimposed on top of the 8HR seismic section. In the 8HR section, bands of strong sub-horizontal reflections in NW at a depth of 38 km, interpreted by Tomek and Hall (1993) as the Moho reflection of the Bohemian Massif, fade out at ~77 km distance, close to the projected location of the S04 Moho step. Similarly, strong lower crustal reflectivity at 20–38 km depth, visible up to a distance of 70–75 km, does not continue beyond the location of the S04 Moho depth change. Taking into account that in this place the profiles run ~20 km away, spatial coincidence of both features (even if approximate) is meaningful and suggests their common origin.

8.2. Magnetotelluric studies

In the area of the Western Carpathians, the magnetotelluric soundings revealed a prominent zone of reversals of the Wiese induction vectors (Wiese, 1965). The individual reversals were perpendicular to the orogen strike, while the axis of the reversal zone ran along the axial part of the whole Western Carpathians. This zone was interpreted as an effect of the Carpathian Conductivity Anomaly produced by more than 1000 km long and ~40 km wide area located in the upper/middle crust (to a depth of ~16 km) consisting of rocks of very low electrical resistivity (~1–4 Ωm). Geographically, the anomaly forms an elongated arcuate area following the Pieniny Klippen Belt in its vicinity (up to few tens of kilometres), though the resolution of determination of such anomalies is limited and decreases with depth due to the nature of potential field methods (Červ et al., 2001; Jankowski et al., 2005).

Jankowski et al. (1985, 2008) explained this conductive zone by a presence of mineralized aqueous fluids contained in the sediments subducted at the European plate margin. Alternative hypothesis links the high conductivity with a high content of organic matter in the sediments subducted to bigger depth, which resulted in metamorphism and graphitization of the organic carbon (e.g., Żytko, 1997). Hübert et al. (2009) discusses that the anomaly with such a low resistivity requires the conductive components (fluids or graphite layers) to be interconnected. In both cases, the anomaly suggests the presence of a long and relatively narrow area beneath or close to the PKB, where sediments were submerged to the upper/middle crustal depths of ~10–16 km and metamorphosed, which most likely reflects the

Miocene subduction/collision processes at the contact of plates (Jankowski et al., 1985, 2008).

8.3. Gravity constraints

Bouguer anomalies are dominated by linear minima that extend from the Eastern Alps along the Carpathians and their northern foreland (Bucha and Blížkovský, 1994). The zone of negative gravity anomalies includes: Carpathian Foredeep, Outer Carpathians, Pieniny Klippen Belt and northern part of the Inner Carpathians (Bielik et al., 2006). Since these anomalies are located close to the area of the abrupt change of the Moho topography, it is advisable to check if gravity modelling gives any additional constraint in modelling of this feature. Hrubcová et al. (2010) calculated a gravity response from two models, a model with the Moho step and a model with a flat Moho. They concluded that there are no substantial differences in the gravity response from both models. The prominent negative velocity anomaly intersecting the S04 profile in the Western Carpathians can be attributed to the presence of thick low-velocity flysch nappes and overlying Neogene sedimentary basins. Consequently, the difference in calculated gravity fields cannot help with discriminating between such extremes at the Moho level.

9. Discussion

Both in the west and north of the Western Carpathians, the origin of the anomalous upper-mantle *Pn* phases is similarly confined to the crust/mantle boundary located beneath the axis of the orogen. Though the phases show different apparent velocity, they represent the structures of a similar origin. Results of modelling document a localized anomaly or an abrupt change of the Moho topography. Such Moho anomalies are traced alongside the Western Carpathian arc and are located in the proximity of the Pieniny Klippen Belt, though their position and shape slightly differ.

9.1. Western side of the Carpathians

At the western edge of the Western Carpathians, the Moho anomaly is similar and dips steeply from about 25–28 km depth to about 36–38 km depth in the north-westward direction (Fig. 10). The Moho anomalies follow the trend of the Pieniny Klippen Belt but they are located ~50 km westward/north-westward from the PKB (Fig. 10). The shape of the Moho topography in the west slightly differs and is influenced by surrounding units at depth. More to the north, along the CEL15 and S04 profiles, we observe an abrupt step-like change of the Moho topography from the southeast to the northwest. More to the south, along the CEL09 profile for both in-line and off-line shot points, the Moho is modelled more as a triangular trough, with Moho sharply dipping from the SE to the NW and rising up in the same direction. The shape of the Moho in these parts is influenced by the increase of crustal thickness for units of the Bohemian Massif: the Moravo-Silesian, Brunovistulian, and the Moldanubian, different in the south and in the north of the massif.

9.2. Northern side of the Carpathians

At the northern rim of the Western Carpathians, the upper-mantle phases were modelled by a local change of the Moho topography forming a rectangular, trough-like anomaly separating areas with similar Moho depths. Such a phenomenon is also documented along the N–S oriented profile V/3K (Uchman, 1975; Zátopek and Beránek, 1975), close to profiles CEL04 and CEL01, where a ~40 km wide Moho trough occurs northwards from the Pieniny Klippen Belt (Fig. 11). It is also visible at the NW–SE trending profile KIII where the Moho discontinuity is disturbed by a vertical step of 6–8 km height (Beránek et al., 1979). Fig. 11 illustrates the character of the Moho anomalies at the northern contact with the European Plate along profiles KIII, CEL01, V/3K, CEL04, and CEL05 (Beránek et al., 1979; Środa, 2010; Środa et al., 2006; Uchman, 1975). Though the shape of the Moho anomaly in these models is a simplified image of the actual structure resulting from different seismic methods and can differ, they all show common feature as is the spatial correlation of the Moho anomalies with the Pieniny Klippen Belt. Środa (2010) studied the upper-mantle arrivals along the profiles CEL01, CEL04, and CEL05 and suggested two models suitable for their interpretation: a model with a small size (of the order of 10 km) velocity anomaly at the Moho level diffracting waves from the upper mantle, and a model with northward inclined reflecting discontinuity of 50–150 km length possibly connected with the crust. In both cases, the anomalous structures were located beneath or close to the PKB.

The diffracting Moho anomaly is more in agreement with the structures modelled along previous DSS profiles. Nevertheless, the position of such presumed diffractor varies. Westward of CEL01 profile it is located ~20 km north of the PKB; along the CEL01 line it is located beneath the PKB; near the crossing of the CEL04 and CEL05 profiles it is located at 20–25 km south of PKB; and finally in the east at the CEL11 line it is located at ~10 km north of the PKB. The latter position of the Moho anomaly is in agreement with the result suggested by Uchman (1975) along profile III.

9.3. Position of the Moho anomalies and the PKB

Local changes in the Moho topography have tectonic significance and their position can trace former plate boundaries at depth. Considering the Pieniny Klippen Belt as a major tectonic unit representing the contact between the European Plate and the ALCAPA at surface, we can relate its position to the position of the Moho anomalies. Fig. 12 displays a projection of the Moho anomalies onto the surface geology to show their location in respect to the PKB. In the western segment of the Carpathian arc, the Moho anomaly runs parallel to the PKB though it is shifted by ~50 km to the NW to the outer side of the Carpathians. Further to the north, the location of the Moho trough in the northern segment of the Western Carpathians follows the trend of the PKB more closely, deviating to the south or north by no more than 25 km. Since the PKB is an important lineament, extending along most of the Western Carpathian arc and is thought to separate the European Plate from the microplate ALCAPA at the surface (e.g., Krobicki et al., 2003; Plašienka et al., 1997), the abrupt change of the Moho topography in its proximity may be related to the collisional deformations near the contact of plates. Since the modelled Moho anomalies can be traced at several places along the Carpathians, we can assume they can be related to the processes of the Carpathian convergence during Tertiary rather than to some older crust-forming processes.

9.4. Analogies with the SE Carpathian structure

The locations of the Moho anomalies in the west follow the trend of the Pieniny Klippen Belt but they are located ~50 km north-westward from the PKB. Some similarity can be found at the opposite end of the orogen, in the SE Carpathians in Romania. There, a substantial change of the Moho depth from seismic studies was also suggested based on the data from the profile VRANCEA 2001 (Hauser et al., 2007). This profile is a 700 km long WNW–ESE trending seismic refraction line and documents thickening of the crust to the ESE from 35 km to 44 km with maximum of the Moho depth located beneath the margin of the outer nappes of the Eastern Carpathians. More importantly, the location of this Moho depth change coincides with the surface projection of the Vrancea seismogenic zone of intra-continental intermediate-depth seismicity (Radulian et al., 2002). This zone is thought to result from the final stages of a subduction/collision process due to the convergence of the Tisza-Dacia and the European Plate during the closure of the Tethys Ocean (e.g., Cloetingh et al., 2004; Gîrbacea and Frisch, 1998;

Popescu and Radulian, 2001; Sperner et al., 2001), where the seismogenic zone is caused by sinking of a lithospheric fragment detached from the European Plate margin delineating a contact of tectonic plates at the upper-mantle depths. The seismicity is also in agreement with regional teleseismic *P*-wave tomography (Bijwaard and Spakman, 2000; Wortel and Spakman, 2000) imaging the presence of a high velocity body beneath Vrancea at a depth interval of about 60–200 km that outlines the seismogenic zone. The contact of the plates at surface is a matter of debates but in some interpretations (e.g., Gîrbacea and Frisch, 1998; Sperner et al., 2004) it is supposed to be located ~80–100 km more to the NW, inwards from the surface projection of the seismogenic zone. Coincidence of the Moho depth change and the seismogenic zone suggests that these features may be related to the contact of plates at depth, which can be regarded as an analogy to the situation at the western side of West Carpathians discussed in this paper.

10. Tectonic implications

The Moho anomalies are visible in several locations following the trend of the orogen, not only along the western part of the Carpathian arc but also at its northern rim (Fig. 12). Such an abrupt change of the Moho topography is quite a prominent phenomenon observed consistently in several places along the Western Carpathians. For this reason, we interpret it as fragments of possibly continuous, arcuate anomalous zone extending along most of the Carpathian belt. From a tectonic point of view, such course of the anomalous zone can suggest that its origin is related to plate convergence that lead to creation of the Western Carpathian mountain chain, i.e., with collisional/transpressional processes during and after the Tertiary subduction.

Comparison of the presented seismic results with previously published seismic models and seismic reflection data, supplemented by present knowledge about geological structure and other geophysical studies points to a new image of the lithosphere at the contact of the European Plate and the ALCAPA microplate. Spatial correlation of the features evidenced by these datasets allows for linking together several phenomena observed at different levels through the crust to the upper mantle (Fig. 12).

At the upper crustal level, the ~600 km long Pieniny Klippen Belt forms a narrow zone of heavy deformations, extending along most of the Western Carpathian orogen. It is considered as a unit resulting from complex tectonic processes, involving compressional and transpressional regime due to oblique convergence and rotation of plates. Therefore, several authors (e.g., Kováč and Hók, 1996; Němčok and Němčok, 1994; Ratschbacher et al., 1993) see the PKB as a surface manifestation of the contact between the European Platform (overridden by Outer Carpathian nappes) and ALCAPA (comprising the Inner Carpathians).

At the upper/middle crustal level (down to about ~10–15 km), a highly conductive zone of the prominent Carpathian conductivity anomaly, extends over ~1000 km along the mountain belt (Jankowski et al., 1985, 2005). Though the resolution of this conductivity anomaly is different and much lower compared to the resolution of the Moho shape obtained from seismic data, the central part of this conductivity anomaly follows roughly the trend of the PKB and, according to Jankowski et al. (1985), it is related to the contact of plates. This zone is interpreted either as composed of sediments with organic content, subducted atop of the European Platform margin to large depths, which resulted in graphitization of the organic carbon. Alternative hypothesis links high conductivity with aqueous fluids released from the subducted sediments (Jankowski et al., 1985, 2008). In both cases, such zone evidences the presence of relatively narrow and long area where sediments were submerged to the middle crustal depths of ~15 km and metamorphosed, which was most likely due to the Miocene subduction/collision processes at the contact of the plates.

At the lower crust/upper-mantle level, the abrupt anomalies of the Moho depth with the amplitude of up to ~15 km are observed along large parts of the orogen, from its western part, near the intersection with CEL09 profile to the eastern part, at the CEL11 profile. This zone of anomalous Moho follows roughly the above-mentioned upper and middle crustal zones of deformations. However, in the western part of the study area (beneath the profiles CEL09, S04) its course deviates from the PKB by as much as ~50 km to the northwest, while in the northern part (profile CEL01) it is close to the PKB or even slightly deviates to the south by some 20–25 km (near the crossing of profiles CEL04 and CEL05). Similar trend is visible along DSS profiles KIII, V/3K and III.

The lateral position of these anomalies delineates a zone affected by deformations at various depths: from the upper/middle crust to the upper mantle, extending along the Western Carpathians. Though their resolution at different crustal levels differs, close spatial correlation among them and their course along the orogenic arc suggest that they all may represent a trace of the same collisional/transpressional processes forming the Carpathian orogen during the Tertiary. Such processes were likely to cause heavy localized deformations and metamorphism in the vicinity of the contact of two lithospheric plates – the European Plate and the ALCAPA. They created an elongated area of shallow and deep crustal deformations, metamorphism or phase changes beneath the Carpathians with horizontal extent, location and intensity of deformations varying along the arc.

Proximity of shallow (PKB), middle-crust (conductivity anomaly), and deep (Moho) deformation zones encourages to delineate the suture at depth. However, such a geometrical correlation would result in a variable orientation of the suture: from a sub-vertical (or steeply dipping) orientation in the north to a west/north-west inclined orientation of the suture in the west (Fig. 12). Such an interpretation might not be consistent with the present view of the south and south-eastward subduction processes driving the Carpathian orogeny in the north and west, respectively (e.g., McCann, 2008; Tomek and Hall, 1993). Nevertheless, the sub-vertical suture was discussed by Lexa and Konečný (1998) and Němčok et al. (1998), who suggested verticalization of the subducting slab and it's tearing during the final collisional stage of the orogen to explain the location of the andesitic arc-type volcanics in the Carpathians.

The western parts exhibit outward offset of the Moho deformations from the PKB zone involving the step-like Moho anomaly and crustal thickness change, different from trough-like Moho anomaly separating crustal fragments of similar thickness in the north. To some extent, a similar situation is discussed at the eastern edge of the SE Carpathians where the crustal thickness changes from the northwest to the southeast (Hauser et al., 2007) and where, according to some interpretations, the suture in the upper mantle is also offset from the location of presumed contact of plates at the surface (e.g., Gîrbacea and Frisch, 1998; Sperner et al., 2004). Assuming such an interpretation, in both cases the Moho depth change occurs outwards from the surface manifestation of the plate contact.

The Tertiary continental collisional events in the Carpathians started in the western part, then continued to the north and finally reached the SE Carpathians most likely with variable character of the collision along the orogen. In the west, where the Carpathian convergence exhibits a large strike-slip component we detect the Moho deformations with the outward offset from the PKB zone. On the other hand, in the north, where mostly compressional component is assumed, the Moho deformations are located beneath the PKB. However, it is not clear why the transpressional tectonics in the west should result in an outward offset of the deep suture relatively to the contact at the surface, different from a near vertical contact in the north with largely compressional tectonics.

11. Conclusions

Anomalous upper-mantle *Pn* phases in data from seismic refraction and wide-angle reflection profiles originate near the contact of the

Western Carpathians with the surrounding units and document localized anomalies of the Moho topography. Their modelling allowed for determination of the shape and precise location of these Moho anomalies. The anomalies are modelled systematically along the Carpathian arc, both in the west and the north. Though their position and shape slightly differ, they are located in the proximity of the Pieniny Klippen Belt, major tectonic unit representing the contact of the ALCAPA and the European Plate at surface. Considering that these anomalies are observed consistently along the Western Carpathians, we interpret them as fragments of possibly continuous, arcuate zone, extending along most of the Western Carpathian belt. Comparison of the Moho anomalies with previously published seismic models and seismic reflection data, supplemented by present knowledge about geology and other geophysical studies enables to delineate the area affected by deformations at various depths: from the upper/middle crust to the upper mantle, extending along the Western Carpathians. Tectonically, such course of the anomalous zone suggests that its origin is related to the lithospheric deformations occurring near the contact of the European Plate and the ALCAPA microplate during the Carpathian orogeny, i.e., it is related to the collisional/transpressional processes during and after the Tertiary.

The present view of the tectonic evolution of the Western Carpathians during the Tertiary assumes the oblique south to southeast-ward subduction of the oceanic lithosphere of the European Plate beneath the units of the ALCAPA (e.g., Plašienka et al., 1997; Tomek and Hall, 1993). However, there is practically no geophysical evidence that would allow positioning of the former plate contact at the Moho level substantially southwards from the PKB, as should be expected in case of assumed south to southeast-dipping subduction. On contrary, complex local Moho anomalies presented in this study document the location of the suture in the immediate vicinity of the PKB rather than far to the south/southeast from the PKB suture. This opens a new consistent view on the suture between the European Plate and the ALCAPA and on the lithospheric structure of the Western Carpathians from the surface to the uppermost mantle.

Acknowledgements

The authors thank the CELEBRATION 2000, ALP 2002, and SUDETES 2003 Working Groups for data acquisition and processing. This research was supported by the Grant Agency of the Czech Republic, Grant No. 13-08971S. The GMT (Wessel and Smith, 1995) and CWP/SU (Cohen and Stockwell, 1997) packages were used for preparation of the figures. The authors are grateful to the editor H. Thybo, A. Malehmir and the anonymous reviewer for their valuable comments and suggestions on the manuscript improvement.

References

Beránek, B., Zátopek, A., 1981. Earth's crust structure in Czechoslovakia and Central Europe by methods of explosion seismology. In: Zátopek, A. (Ed.), Geophysical syntheses in Czechoslovakia. Veda, Bratislava, pp. 253–264.

Beránek, B., Leško, B., Mayerová, M., 1979. Interpretation of seismic measurements along the Trans-Carpathian profile K III. In: Vaněk, J., Babuška, V., Plančat, J. (Eds.), Geodynamic Investigation in Czechoslovakia. Veda, Bratislava, pp. 201–210.

Bielik, M., Šefara, J., Kováč, M., Bezák, V., Plašienka, D., 2004. The Western Carpathians — interaction of Hercynian and Alpine processes. Tectonophysics 393, 63–86.

Bielik, M., Kloska, K., Meurers, B., Švancara, J., Wybraniec, S., CELEBRATION 2000 Potential Field Working Group, 2006. Gravity anomaly map of the CELEBRATION 2000 region. Geol. Carpath. 57 (3), 145–156.

Bijwaard, H., Spakman, W., 2000. Non-linear global P-wave tomography by iterated linearized inversion. Geophys. J. Int. 141, 71–82.

Birkenmajer, K., 1986. Stages of structural evolution of the Pieniny Klippen Belt, Carpathians. Stud. Geol. Pol. 88, 7–32.

Brückl, E., Bodoky, T., Hegedűs, E., Hrubcová, P., Gosar, A., Grad, M., Guterch, A., Hajnal, Z., Keller, G.R., Špičák, A., Sumanovac, F., Thybo, H., Weber, F., ALP 2002 Working Group, 2003. ALP 2002 seismic experiment. Stud. Geophys. Geod. 47, 671–679. http://dx.doi.org/10.1023/A:1024780022139.

Brückl, E., Bleibinhaus, F., Gosar, A., Grad, M., Guterch, A., Hrubcová, P., Keller, G.R., Majdański, M., Sumanovac, F., Tiira, T., Yliniemi, J., Hegedűs, E., Thybo, H., 2007. Crustal structure due to collisional and escape tectonics in the Eastern Alps region based on profiles Alp01 and Alp02 from the ALP 2002 seismic experiment. J. Geophys. Res. 112, B06308. http://dx.doi.org/10.1029/2006JB004687.

Bucha, V., Blížkovský, M. (Eds.), 1994. Crustal structure of the Bohemian Massif and the West Carpathians. Academia Praha.

Červ, V., Kováčiková, S., Pek, J., Pěčová, J., Praus, O., 2001. Geoelectrical structure across the Bohemian Massif and the transition zone to the West Carpathians. Tectonophysics 332, 201–210.

Červený, V., Pšenčík, I., 1984. SEIS83 — numerical modelling of seismic wave fields in 2-D laterally varying layered structures by the ray method. In: Engdal, E.R. (Ed.), Documentation of Earthquake Algorithms. Rep. SE-35, World Data Cent. A for Solid Earth Geophysics, Boulder, Colo, pp. 36–40.

Cloetingh, S.A.P.L., Burov, E., Matenco, L., Toussaint, G., Bertotti, G., Andriessen, P.A.M., Wortel, M.J.R., Spakman, W., 2004. Thermo-mechanical controls on the model of continental collision in the SE Carpathians (Romania). Earth Planet. Sci. Lett. 218, 57–76.

Cohen, J.K., Stockwell Jr., J.W., 1997. CWP/SU: Seismic Unix Release 30: a free package for seismic research and processing. Center for Wave Phenomena, Colorado School of Mines.

Gîrbacea, R., Frisch, W., 1998. Slab in the wrong place: lower lithospheric mantle delamination in the last stage of the Eastern Carpathian subduction retreat. Geology 26 (7), 611–614.

Golonka, J., Krobicki, M., 2004. Jurassic paleogeography of the Pieniny and Outer Carpathian basins. Riv. Ital. Paleontol. Stratigr. 110, 5–14.

Grad, M., Špičák, A., Keller, G.R., Guterch, A., Brož, M., Hegedűs, E., Working Group, 2003a. SUDETES 2003 seismic experiment. Stud. Geophys. Geod. 47, 681–689. http://dx.doi.org/10.1023/A:1024732206210.

Grad, M., Jensen, S.L., Keller, G.R., Guterch, A., Thybo, H., Janik, T., Tiira, T., Yliniemi, J., Luosto, U., Motuza, G., Nasedkin, V., Czuba, W., Gaczyński, E., Oeroda, P., Miller, K.C., Wilde-Piórko, M., Komminaho, K., Jacyna, J., Korabliova, L., 2003b. Crustal structure of the Trans-European Suture Zone region along Polonaise'97 seismic profile P4. J. Geophys. Res. 108 (B11).

Grad, M., Guterch, A., Keller, G.R., Janik, T., Hegedűs, E., Vozár, J., Ślączka, A., Tiira, T., Liniemi, J., 2006. Lithospheric structure beneath trans-Carpathian transect from Precambrian platform to Pannonian basin: CELEBRATION 2000 seismic profile CEL05. J. Geophys. Res. 111, B03301. http://dx.doi.org/10.1029/2005JB003647.

Guterch, A., Grad, M., Keller, G.R., Posgay, K., Vozár, J., Špičák, A., Brueckl, E., Hajnal, Z., Thybo, H., Selvi, O., CELEBRATION 2000 Experiment Team, 2003. CELEBRATION 2000 Seismic Experiment. Stud. Geophys. Geod. 47, 659–670.

Hansen, T.M., Jacobsen, B.H., 2002. Efficient finite difference waveform modelling of selected phases using a moving zone. Comput. Geosci. 28 (7), 819–826.

Hauser, F., Raileanu, V., Fielitz, W., Dinu, C., Landes, M., Bala, A., Prodehl, C., 2007. Seismic crustal structure between the Transylvanian Basin and the Black Sea, Romania. Tectonophysics 430, 1–25. http://dx.doi.org/10.1016/j.tecto.2006.10.005.

Hirn, A., Lepine, J.C., Jobert, G., Sapin, M., Wittlinger, G., Xin, X.Z., Yuan, G.E., Jing, W.X., Wen, T.J., Bai, X.S., Pandey, M.R., Tater, J.M., 1984a. Crustal structure and variability of the Himalayan border of Tibet. Nature 307 (5946), 23–25.

Hirn, A., Nercessian, A., Sapin, M., Jobert, G., Xin, X.Z., Yuan, G.E., Yuan, L.D., Wen, T.J., 1984b. Lhasa block and bordering suture-continuation of a 500 km Moho traverse through Tibet. Nature 307 (5946), 25–27.

Hrubcová, P., Geissler, W., 2009. The crust–mantle transition and the Moho beneath the Vogtland/West Bohemian region in the light of different seismic methods. Stud. Geophys. Geod. 53, 275–294.

Hrubcová, P., Środa, P., Špičák, A., Guterch, A., Grad, M., Keller, G.R., Brückl, E., Thybo, H., 2005. Crustal and uppermost mantle structure of the Bohemian Massif based on data from CELEBRATION 2000 Experiment. J. Geophys. Res. 110, B11305. http://dx.doi.org/10.1029/2004JB003080.

Hrubcová, P., Środa, P., CELEBRATION 2000 Working Group, 2008. Crustal structure at the easternmost termination of the Variscan belt based on CELEBRATION 2000 and ALP 2002 data. Tectonophysics 460, 55–75. http://dx.doi.org/10.1016/j.tecto.2008.07.009.

Hrubcová, P., Środa, P., Grad, M., Geissler, W.H., Guterch, A., Vozár, J., Hegedűs, E., Sudetes 2003 Working Group, 2010. From the Variscan to the Alpine Orogeny: Crustal structure of the Bohemian Massif and Western Carpathians in the light of the SUDETES 2003 seismic data. Geophys. J. Int. 183, 611–633. http://dx.doi.org/10.1111/j.1365-246X.2010.04766.

Hrušecký, I., Plašienka, D., Pospíšil, L., 2006. The Carpathians and their foreland: geology and hydrocarbon resources. In: Golonka, J., Pícha, F.J. (Eds.), The Carpathians and Their ForelandAAPG Memoir 84. American Association of Petroleum Geologists, pp. 717–727. http://dx.doi.org/10.1306/985625M843082.

Hübert, J., Malehmir, A., Smirnow, M., Tryggvason, A., Pedersen, L.B., 2009. MT measurements in the western part of the Paleoproterozoic Skellefte Ore District, Northern Sweden: A contribution to an integrated geophysical study. Tectonophysics 475, 493–502. http://dx.doi.org/10.1016/j.tecto.2009.06.011.

Janik, T., Grad, M., Guterch, A., CELEBRATION 2000 Working Group, 2009. Seismic structure of the lithosphere between the East European Craton and the Carpathians from the net of CELEBRATION 2000 profiles in SE Poland. Geol. Quat. 53 (1), 141–158.

Jankowski, J., Tarłowski, Z., Praus, O., Pěčová, J., Petr, V., 1985. The results of deep geomagnetic soundings in the West Carpathians. Geophys. J. R. Astron. Soc. 80, 561–574.

Jankowski, J., Praus, O., Jóźwiak, W., 2005. Carpathian anomaly of electrical conductivity; History of its discovery and interpretation. *Publs. Inst. Geophys. Pol. Acad. Sc.*, C-95 386, pp. 17–27.

Jankowski, J., Jóźwiak, W., Vozár, J., 2008. Arguments for ionic nature of the Carpathian electric conductivity anomaly. Acta Geophys. 56, 455–465. http://dx.doi.org/10.2478/s11600-008-0004-3.

Jensen, S.L., Thybo, H., the POLONAISE'97 Working Group, 2002. Moho topography and lower crustal wide-angle reflectivity around the TESZ in southern Scandinavia and northeastern Europe. Tectonophysics 360, 187–213.
Komminaho, K., 1997. Software manual for programs MODEL and XRAYS — a graphical interface for SEIS83 program package. Rep. 20, 31. Dep. of Geophysics Univ. of Oulu, Oulu, Finland.
Kováč, P., Hók, J., 1996. Tertiary development of the western part of Klippen Belt. Slovak Geol. Mag. 2/96, 137–149.
Krobicki, M., Golonka, J., Aubrecht, R., 2003. Pieniny Klippen Belt: general geology and geodynamic evolution. In: Golonka, J., Lewandowski, M. (Eds.), Geology, geophysics, geothermics and deep structure of the West Carpathians and their basement.
Lexa, J., Konečný, V., 1998. Geodynamic aspects of the neogene to quaternary volcanism. In: Rákus, M. (Ed.), Geodynamic development of theWestern Carpathians, GSSR, Bratislava, pp. 143–154.
Malinowski, M., CELEBRATION 2000 Working Group, 2003. Seismic crustal structure of the Alpine–Pannonian area revealed by the CELEBRATION 2000 experiment. Profiles CEL08 and CEL07, EGS-AGU-EUG Joint Assembly, Nice, France.
The Geology of Central Europe. In: McCann, T. (Ed.), Mesozoic and Cenozoic vol. 2. Geological Society of London.
Němčok, M., Němčok, J., 1994. Late Cretaceous deformation of the Pieniny Klippen Belt West Carpathians. Tectonophysics 239, 81–109.
Němčok, M., Pospíšil, L., Lexa, J., Donelick, R.A., 1998. Tertiary subduction and slab breakoff model of the Carpathian–Pannonian region. Tectonophysics 295, 307–340.
Plašienka, D., Grecula, P., Putiš, M., Kováč, M., Hovorka, D., 1997. Evolution and structure of the Western Carpathians: an overview. In: Grecula, P., Hovorka, D., Putiš, M. (Eds.), Geological evolution of the Western Carpathians. Mineralia Slovaca, Bratislava, pp. 1–24.
Popescu, E., Radulian, M., 2001. Source characteristics of the seismic sequences in the Eastern Carpathians foredeep region (Romania). Tectonophysics 338, 325–337.
Radulian, M., Popescu, E., Bala, A., Utale, A., 2002. Catalog of fault plane solutions for the earthquakes occurred on the Romanian territory. Rom. J. Phys. 47, 663–685.
Ratschbacher, L., Linzer, H.G., Moser, F., Strusievicz, R.O., Bede1ean,, H., Har, N., Mogos, P.A., 1993. Cretaceous to Miocene thrusting and wrenching along the central south Carpathians due to a comer effect during collision and orocline formation. Tectonics 12, 855–873.
Sperner, B., Lorenz, F., Bonjer, K., Hettel, S., Müller, B., Wenzel, F., 2001. Slab break-off — abrupt cut or gradual detachment? New insights from the Vrancea region (SE Carpathians, Romania). Terra Nova 13, 172–179.
Sperner, B., Ioane, D., Lilly, R.J., 2004. Slab behavior and its surface expression: new insights from gravity modelling in the SE-Carpathians. Tectonophysics 382, 51–84.
Środa, P., 2010. The bright spot in the West Carpathian upper mantle: a trace of the Tertiary plate collision and a caveat for a seismologist. Geophys. J. Int. 182, 1–10. http://dx.doi.org/10.1111/j.1365-246X.2010.04595.x.
Środa, P., Czuba, W., Grad, M., Guterch, A., Tokarski, A.K., Janik, T., Rauch, M., Keller, G.R., Hegedűs, E., Vozár, J., CELEBRATION 2000 Working Group, 2006. Crustal and upper mantle structure of the Western Carpathians from CELEBRATION 2000 profiles CEL01 and CEL04: seismic models and geological implications. Geophys. J. Int. 167, 737–760. http://dx.doi.org/10.1111/j.1365-246X.2006.03104.
Thybo, H., Nielsen, C.A., 2012. Seismic velocity structure of crustal intrusions in the Danish Basin. Tectonophysics 572–573, 64–75. http://dx.doi.org/10.1016/j.tecto.2011.11.019.
Tomek, Č., 1993. Deep crustal structure beneath the central and inner West Carpathians. Tectonophysics 226, 417–431.
Tomek, Č., Hall, J., 1993. Subducted continental margin imaged in the Carpathians of Czechoslovakia. Geology 21, 535–538.
Uchman, J., 1975. Tectonic characteristics of the region of International Profile V of deep seismic sounding in the Outer Carpathians and Foreland. Publs. Inst. Geoph. Pol. Ac. Sci. 82, pp. 111–118.
Vozár, J., Szalaiová, V., Šantavý, J., 1998. Interpretation of the western Carpathian deep structures on the basis of gravimetric and seismic sections. In: Rákus, M. (Ed.), Geodynamic Development of the Western Carpathians. Geological Survey of the Slovak Republic, Bratislava, Slovakia, pp. 241–257.
Vozár, J., Šantavý, J., Potfaj, M., Szalaiová, V., Scholtz, P., Tomek, Č., Šefara, J., Machková, N., Hnojem, I., Šály, B., Pereszlényi, M., Hrušecký, I., Hlavatý, I., Juřena, V., Rudinec, R., Magyar, J., Slávik, M., 1999. Atlas of deep reflection seismic profiles of the Western Carpathians and their interpretation. *Geol. Survey of Slovak Rep.*, Bratislava.
Wessel, P., Smith, W.H.F., 1995. New version of Generic Mapping Tools released, *EOS*. EOS Trans. Am. Geophys. Union 76, 329.
Wiese, H., 1965. Geomagnetische Induktionspfeile in der CSRR hervorgerufen durch grossraumige elektrische Leitfahigkeitsstrukturen. Stud. Geophys. Geod. 9, 415–419.
Wortel, M.J.R., Spakman, W., 2000. Subduction and slab detachment in the Mediterranean–Carpathian region. Science 290, 1910–1917.
Zátopek, A., Beránek, B., 1975. Geophysical synthesis and crustal structure in central Europe. Stud. Geophys. Geod. 19, 121–133.
Zelt, C.A., 1994. ZPLOT — an interactive plotting and picking program for seismic data. Bullard Lab., Univ. of Cambridge, Cambridge UK.
Żytko, K., 1997. Electrical conductivity anomaly of the Northern Carpathians and the deep structure of the orogen. Ann. Soc. Geol. Pol. 67 (1), 25–43.